Halo Current Analysis of Center Stack

NSTXU-Calc- 133-05-01

Rev 0: September 15 2011

Rev 1: December 16, 2013

Prepared By:

Art Brooks
Digitally signed by Art Brooks
DN: cn=Art Brooks, o=PPPL, ou=Engineering, email=abrooks@pppl.gov, c=US
Date: 2014.05.15 13:21:45 -04'00'

Art Brooks, Engineering Analyst

Reviewed By:

Peter H. Titus
Digitally signed by Peter H. Titus
DN: cn=Peter H. Titus, o, ou=Princeton Plasma Physics Laboratory, email=ptitus@pppl.gov, c=US
Date: 2014.06.04 07:27:12 -04'00'

Peter Titus, Branch Head, Engineering Analysis Division

Reviewed By:

Phil Heitenroeder
Digitally signed by Phil Heitenroeder
DN: cn=Phil Heitenroeder, o=PPPL, ou=Mechanical Eng. Div., email=pheitzen@pppl.gov, c=US
Date: 2014.06.04 11:58:58 -04'00'

Phil Heitzenroeder, Head, Mechanical Engineering

Halo Current Analysis of NSTX CS

PPPL Calculation Form

Calculation # **NSTXU-CALC- 133-05-01** Revision# 1 WP #____ (ENG-032)

Purpose of Calculation: (Define why the calculation is being performed.)

Estimate the inductive effects during a halo current strike on currents, forces and stresses.

References (List any source of design information including computer program titles and revision levels.)

1) NSTX_CSU-RQMTS-GRD General Requirements Documents, Rev 3
2) Design Point Spreadsheet "NSTX_CS_Upgrade_100504.xls"
3) ProE Model of Center Stack Tiles - aj_center_case_analysis_rev2.asm
4) Spreadsheet of Disruption Data - Disruption_scenario_currents_v2.xlsx, by Jon Menard, received 7/2/2010
5) Discussions with Stefan Gerhardt on modeling of halo currents for NSTX
6) Bellows Qualification Calc # NSTXU CALC 133-10-00, Peter Rogoff'
7) NSTX Upgrade Center Stack Casing and Lower Skirt Stress Summary NSTXU-CALC-133-03-00 Peter Titus
8) Email Sept 9 2011 containing recommendations for damping values, including Regulatory Guide 1.61 as an attachment. Included in Attachment A
9) MODELLING OF THE TOROIDAL ASYMMETRY OF POLOIDAL HALO CURRENTS IN CONDUCTING STRUCTURES N. POMPHREY, J.M. BIALEK_, W. PARK, Princeton Plasma Physics Laboratory, Princeton University, Princeton, New Jersey, NJ

Assumptions (Identify all assumptions made as part of this calculation.)

Initially current is flowing in the outer region of the plasma (herein modeled as a set of TF like coils) with a portion of it (ie the inboard leg) in close proximity to the CS. This portion in close proximity is driven to zero as the current it was carrying is injected at the top and removed from the bottom of CS and returned thru the outboard leg of the plasma. This is evaluated for a slow, fast and medium current quench halo strikes.

Calculation (Calculation is either documented here or attached)

See body of this report.

Conclusion (Specify whether or not the purpose of the calculation was accomplished.)

The results presented here show the inductive effects to be potentially significant for the halo model assumptions presented. The impact should be further quantified by investigating the dynamic impact on the loads found on the CS. There is a miss-match between the GRD and what was used in the calculation, and because of the uncertainty in the halo current TPF and Halo fraction, restraints were added to the top to limit moments at the base and loads at the bellows.

Halo Current Analysis of NSTX CS

Note: Per P. Titus e-mail of 10/25/2011, *"This calculation does not have the final loads, but based on this calculation and discussions with J Menard, S Gerhardt, and Jim Chrzanowski, we are putting shims between PF1b and 1c mandrels at the top of the casing to limit the loads at the base and bellows.This is a valid conclusion in the calc and it can be signed out."*

In Rev 1, the reactions at the shims and the pedestal were recalculated with a compliance added that models the G-10 ring between the TF flags and the casing skirt base. Loads and moments were reduced and these lower loads were incorporated in the centerstack casing calculation.

Cognizant Engineer's printed name, signature, and date

Phil Heitenroeder

Digitally signed by Phil Heitenroeder
DN: cn=Phil Heitenroeder, o=PPPL, ou=Mechanical Eng. Div., email=pheitzen@pppl.gov, c=US
Date: 2014.06.04 11:58:14 -04'00'

I have reviewed this calculation and, to my professional satisfaction, it is properly performed and correct.

Checker's printed name, signature, and date

Peter H. Titus

Digitally signed by Peter H. Titus
DN: cn=Peter H. Titus, o, ou=Princeton Plasma Physics Laboratory, email=ptitus@pppl.gov, c=US
Date: 2014.06.04 07:27:36 -04'00'

Halo Current Analysis of NSTX CS

Executive Summary

An analysis was done to estimate the inductive effects during a halo current strike. Previous analyses and guidance have assumed the flow of halo current thru structures is resistively distributed. The halo currents were modeled as a current source entering at one poloidal location and leaving at another. This assumed resistive distribution results in a potentially non conservative prediction of EM loads on the structures. Results presented herein show that the time constant for establishing the halo current flow is fairly long relative to the fast disruption timescale resulting in less current redistribution and higher forces than for a resistive solution (or slow quench).

A dynamic stress calculation with damping is also presented which calculates the displacements and reactions at the bellows, the reactions at the base support and the CS stresses.

The results presented here showed the inductive effects to be significant for the halo model assumptions presented. The slow quench (100 ms) has a fairly resistive response leading to more current redistribution, lowering the toroidal peaking factor to 5% at the midplane, and lower net radial forces. The fast quench (1 ms) shows much less current redistribution with the toroidal peaking factor the midplane still 22% and much higher net radial forces (140kN). The decision by physics to apply the TPF to the midplane and not the strike point drove the net radial force up to 250 kN. The max lateral displacement at the bellows is 0.5mm and reactors a small part of the applied load whereas the base support must be capable of reacting the full 250kN load. The stresses are shown to be fairly independent of the scenario. At the revised loading the max tresca stress is 73 MPa, well within allowables.

Adding the compliant G10 plate and structure sitting on the TF flags reduces the moment (now measure at the G10, z=-2.7m) to a peak of 95 kN-m during the dynamic response. The net lateral force drops to 180 kN. The bellows/bumper reaction drop slightly to 32 kN and again is not in phase with the reaction load at the base (see figures)

The peak vertical load at the interface of the base of the CS and top of the lower support is lower (~60 kN) than at the bottom of the lower support (~80 kN). The moments are about the same (~95 kN-m) but occur at different times. The numbers are extracted using fsum on the interface nodes with the lower support elements and are the total force (static + inertial + damping).

Introduction

The current distribution in the plasma during a disruption is fairly complicated. The current in general follows the helical magnetic field lines. From an engineering viewpoint it is convenient to decompose the distribution into toroidal and poloidal currents. Most disruption analyses concerns itself with the rapid movement and decay of the toroidal

currents. Here there is only an inductive coupling between the toroidal currents representing the plasma and the induced eddy currents in the structures. Where there are poloidally electrical continuous structures surrounding the plasma, the inductive coupling of the poloidal currents (both large scale and small - ie the spiraling of electrons around field lines), characterized by toroidal flux changes in the plasmas, can have a significant impact as well. And when the plasma makes contact with the structure, a portion of the current flowing in the plasma is intercepted and effectively shorted thru the structure. It is these currents that are addressed here. While they do not occur alone, it is useful to separate them to try and understand their impact. Further, the halo is assumed to occur due to a plasma instability that distorts the shape and position of the plasma causing an asymmetry of the intercepted halo currents.

Halo Current Analysis of NSTX CS

Assumptions

To estimate the inductive effects it is necessary to know the conditions that precede a halo current strike. The assumptions made here is that initially current is flowing in the outer region of the plasma (herein modeled as a set of TF like coils) with a portion of it (ie the inboard leg) in close proximity to the CS. This portion in close proximity is driven to zero as the current it was carrying is injected at the top and removed from the bottom of CS and returned thru the outboard leg of the plasma. The current waveform for each disruption is given in Ref 4.

Since the current that is driven in the structure comes from shorting the halo in the plasma, for short time scale this should produce currents in the structure that very nearly parallel the currents in the shorted halo to preserve flux. This current then redistributes on the time scale of the structure to a resistive distribution. For a fast halo strike with a toroidal peaking factor of 1.35 this implies that immediately after current strikes the CS the vertical current flow thru the CS also has a toroidal peaking factor of 1.35 then redistributes to a resistive distribution where the peaking factor between the halo entry and exit points has been found to be much closer to one. This is significant because the net force on the CS from the interaction of the vertical halo currents with the TF field is zero in a region where the peaking factor is 1 (uniform current density) since forces on opposites sides of the CS would balance. For non uniform currents there is a force imbalance and a resulting net force.

Method of Analysis

An ANSYS 3D Electromagnetic Model was generated of the CS and excited by a set of TF like coils representing the plasma halo region as shown below (a half plane of vacuum elements is removed to expose the interior).

Halo Current Analysis of NSTX CS

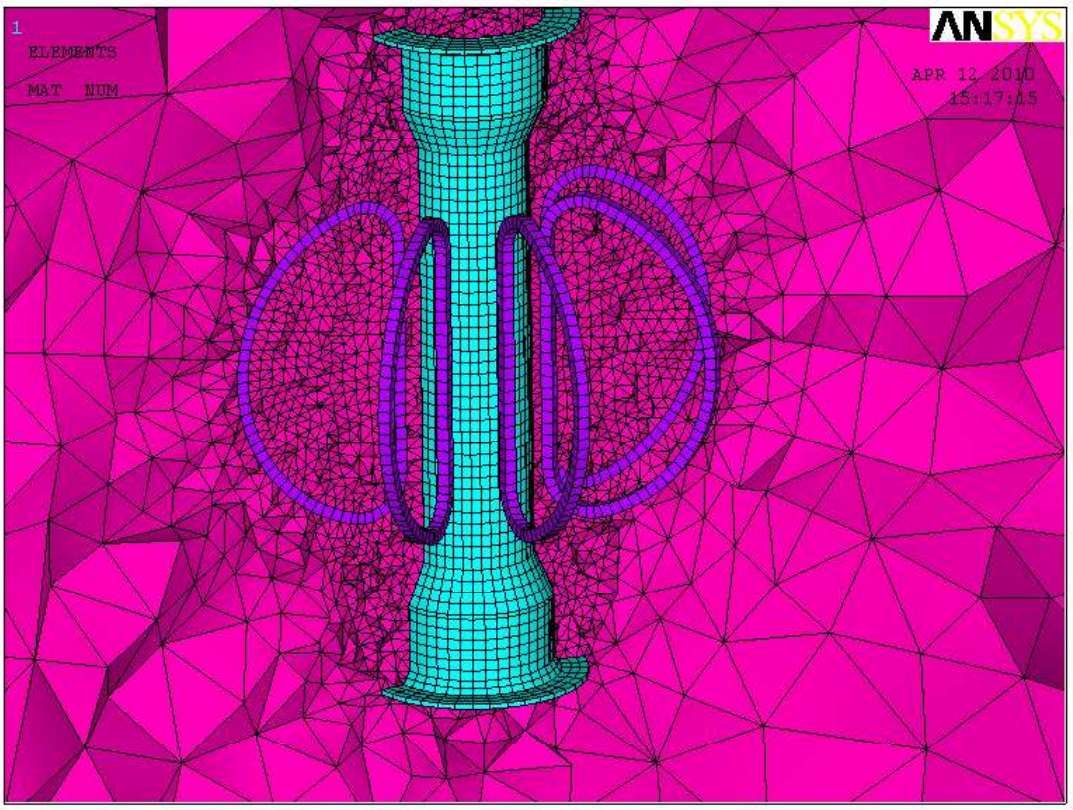

Figure 1 ANSYS Mesh

The model uses solid97 elements with eddy current capability activated for the CS. The CS is assumed to be inconel with a resistivity of 130.e-8 ohm-m. The coils representing the plasma halo are assumed to carry an initial current distribution totaling 400 kA (2 MA plasma current with 20% HCF) but modulated to provided a 35% toroidal peak factor, TPF (from Ref 5: TPF=1+.07/HCF) or a j=javg*(1+.35*cos(phi)) distribution. The halo current strike is assumed to occur, as specified in Ref 4, as a triangular waveform which starts at the beginning of the current quench, peaks in the middle and returns to zero at the end. This analysis focuses on the three halo current scenarios associated with a centered disruption which load up the most of the center stack. These are excerpted below from Ref 4.

Disruption scenario description	Initial Ip [MA]	Drift time [s]	Quench time [s]	Halo fraction f_h	Toroidal Peaking Factor
Inward drift to CS, very slow quench, halo	2	0.01	0.1	0.2	1.35
Inward drift to CS, fast quench, halo	2	0.01	0.001	0.2	1.35
Inward drift to CS, medium quench, halo	2	0.01	0.004	0.2	1.35

From a modeling standpoint the current in the plasma halo is ramped to zero while at the same time injecting equal current into the neighboring CS structure at z=+/- 0.6m to

simulate the transfer of current from the plasma halo to the CS structure as shown below:

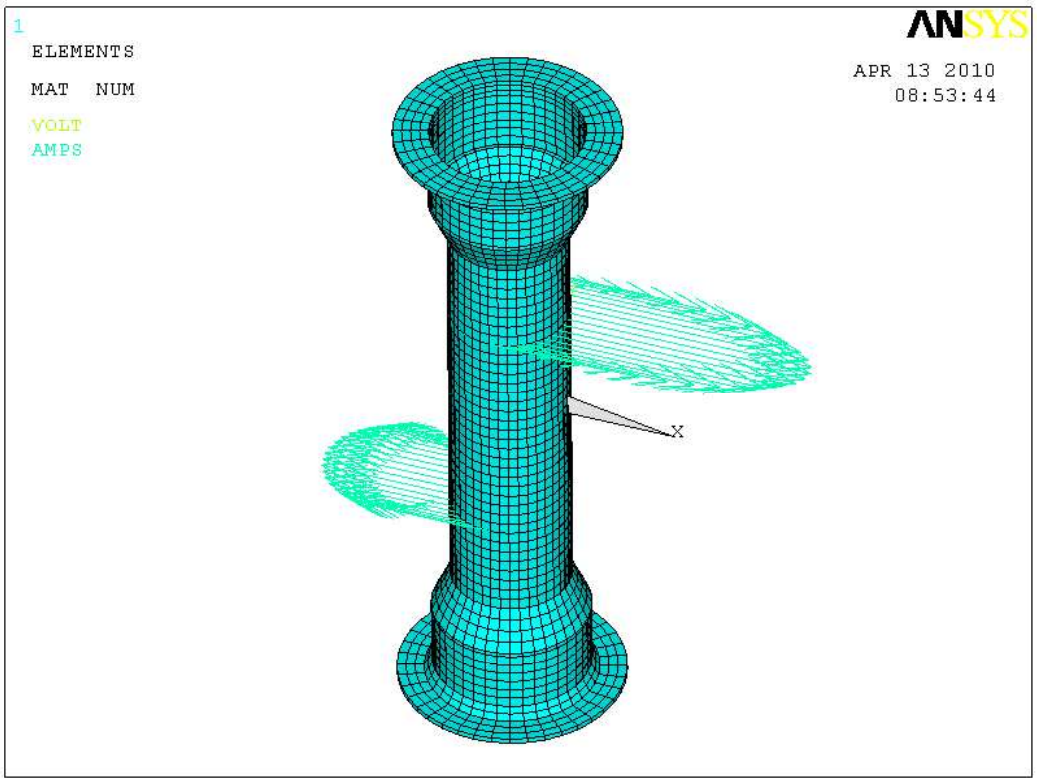

Figure 2 CS Halo Current Inject Distribution

The injected halo current relative distribution is assumed to persist while the eddy currents in the CS redistribute over time.

Results

Preliminary analysis was done with a step function for the halo currents and TPF=2, held for the duration of the simulation. From these results, shown below, a time constant for current redistribution was calculated to be ~ 1.3 ms. The halo currents flowing in the CS change significantly from the initial inductive distribution to their final resistive distribution. The plots below show the distribution of currents in the entire CS and then in just a slice thru the midplane where the variation is more apparent.

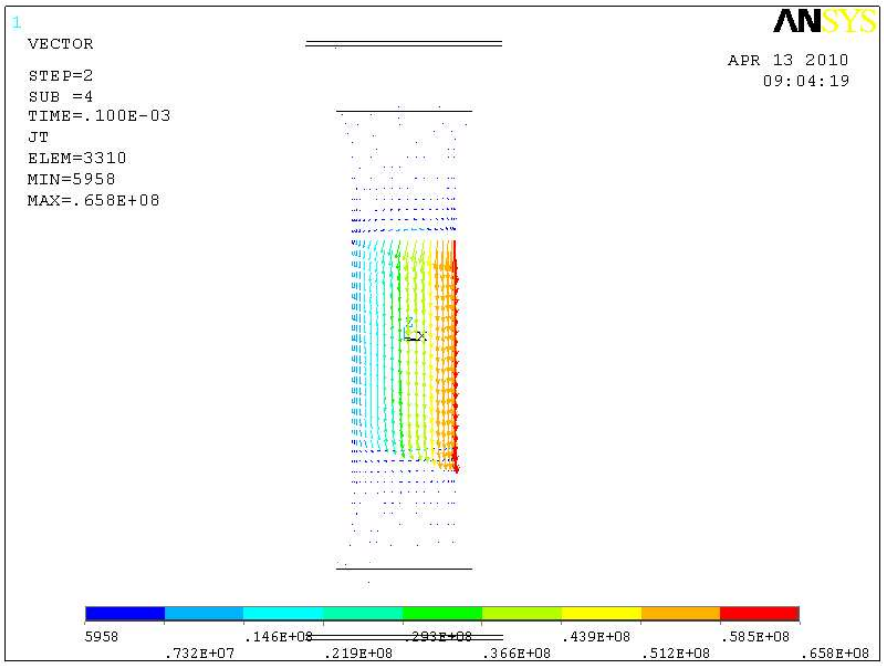

Figure 3 Inductive Distribution immediately following a stepped function halo current strike on the CS. Distribution mirror initial assumed plasma distribution

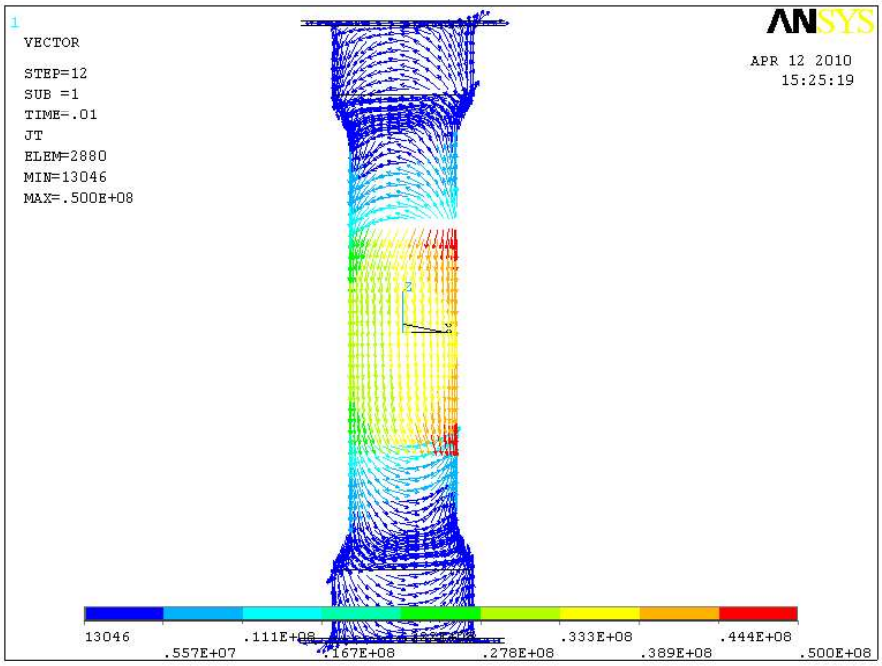

Figure 4 Resistive distribution 10ms after halo strike

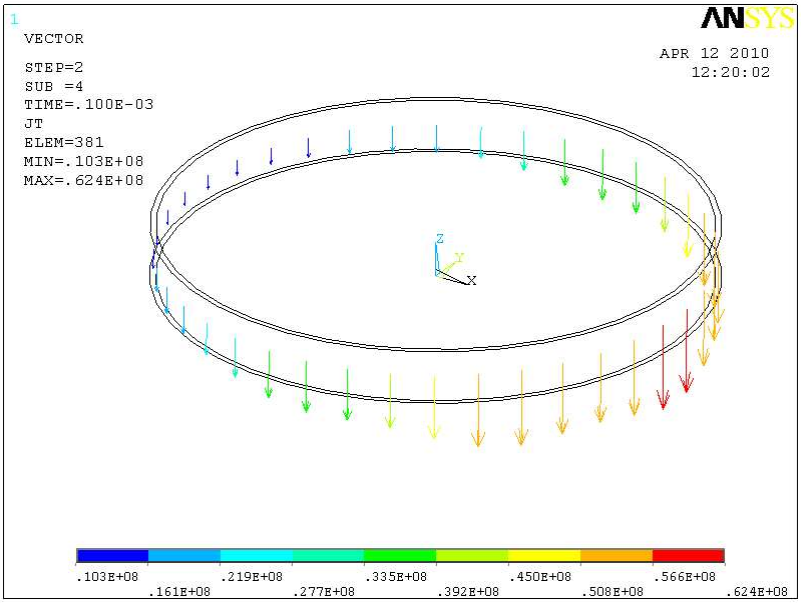

Figure 5 Inductive Distribution immediately following the stepped halo current strike on the CS shows large distribution in current density consistent with a toroidal peaking factor of 2 source.

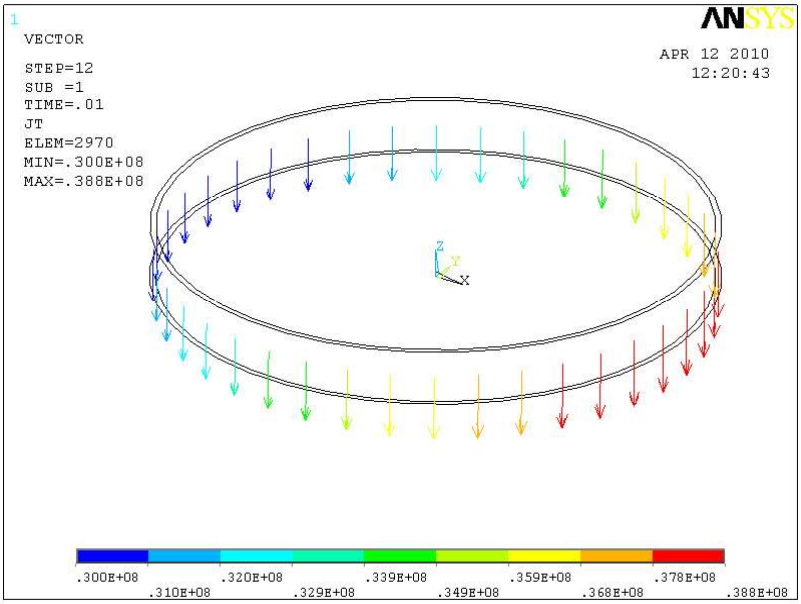

Figure 6 Resistive distribution 10 ms after halo current strike shows fairly small residual peaking factor at midplane.

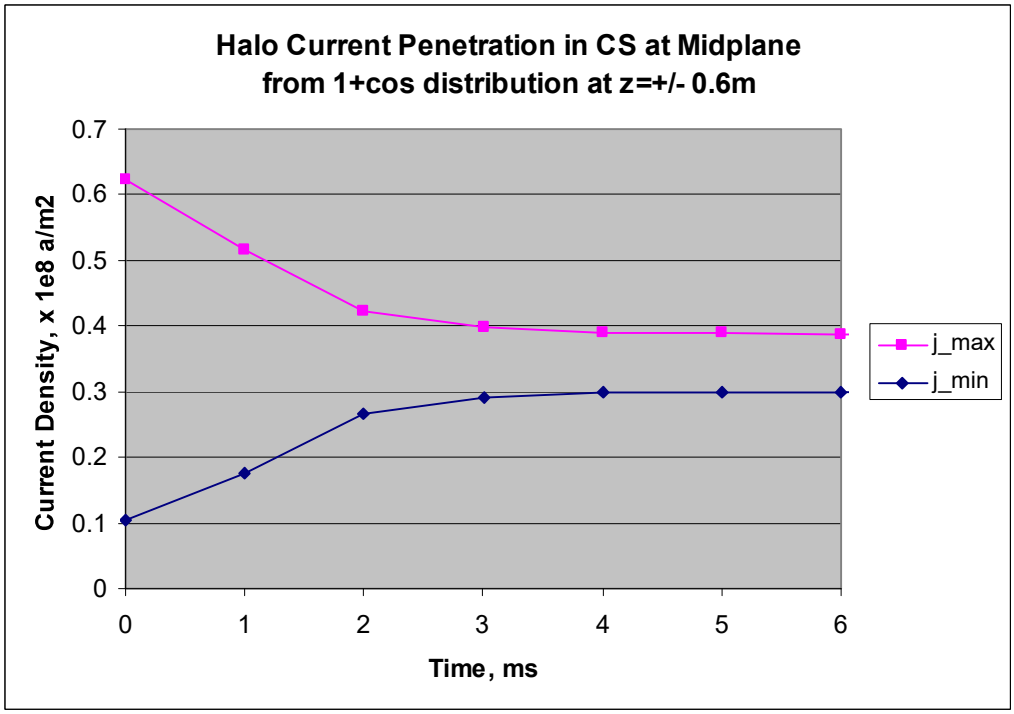

Figure 7 Penetration of the Halo current in the CS measured at the midplane.

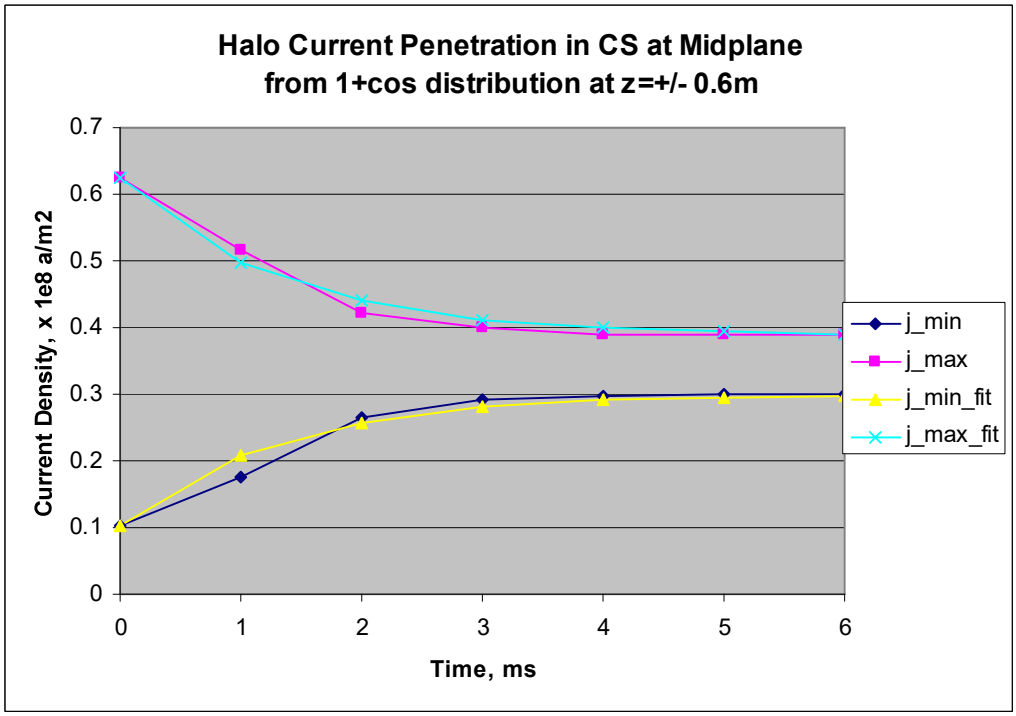

Figure 8 Same data with a simple exponential decay best fitted with a time constant 1.31 ms.

Halo Current Analysis of NSTX CS

Results for the design basis triangular waveform halo current scenarios are summarized below with a resistive distribution given for comparison. The highest current peaking factor occurs for the fast quench as would be expected. This produces the highest lateral forces as the vertical current flow crosses the TF field.

Maximum Net Lateral Force, Kg	
slow quench	-4216
fast	146000
med	73376
resistive	-5382

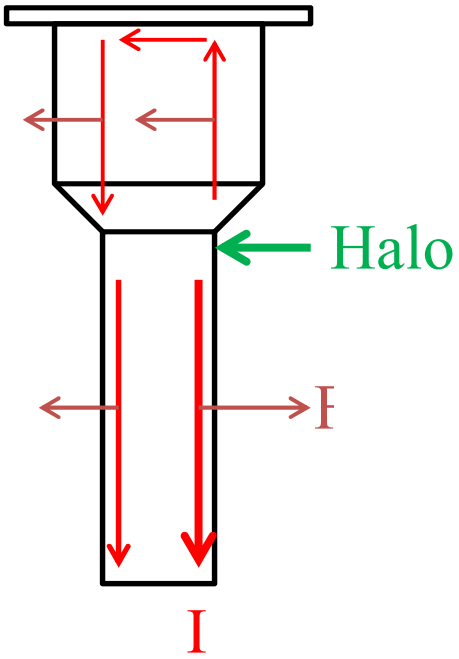

Note since the halo current does not just flow from inlet to outlet strike points across the midplane but also circulates into the upper and lower portions the of the CS redistributing the currents, the Toroidal Peaking Factor is lowered even just below the strike point where 35% peaking might have been be expected. This also reduces lateral forces, particularly in the slow or resistive scenarios, where the forces on the upper and lower portions more than cancel out the forces in the mid section. This effect is illustrated at the left.

Halo Current Analysis of NSTX CS

Current Disribution for Halo Current Scenarios					
Ihalo=400kA, TPF=1.35					
slow quench, tup=.05 (end of ramp up)			j, e8 a/m2		
		min	max	avg	TPF-1
	Top	0.289	0.400	0.345	0.161
	Halfway	0.321	0.368	0.345	0.068
	Midplane	0.327	0.361	0.344	0.049
fast quench, tup=.0005 (end of ramp up)			j, e8 a/m2		
		min	max	avg	TPF-1
	Top	0.255	0.440	0.348	0.266
	Halfway	0.270	0.428	0.349	0.226
	Midplane	0.274	0.424	0.349	0.215
medium quench, tup=.002 (end of ramp up)			j, e8 a/m2		
		min	max	avg	TPF-1
	Top	0.273	0.418	0.346	0.210
	Halfway	0.298	0.394	0.346	0.139
	Midplane	0.303	0.389	0.346	0.124
Resistive			j, e8 a/m2		
		min	max	avg	TPF-1
	Top	0.290	0.399	0.345	0.158
	Halfway	0.322	0.366	0.344	0.064
	Midplane	0.329	0.359	0.344	0.044

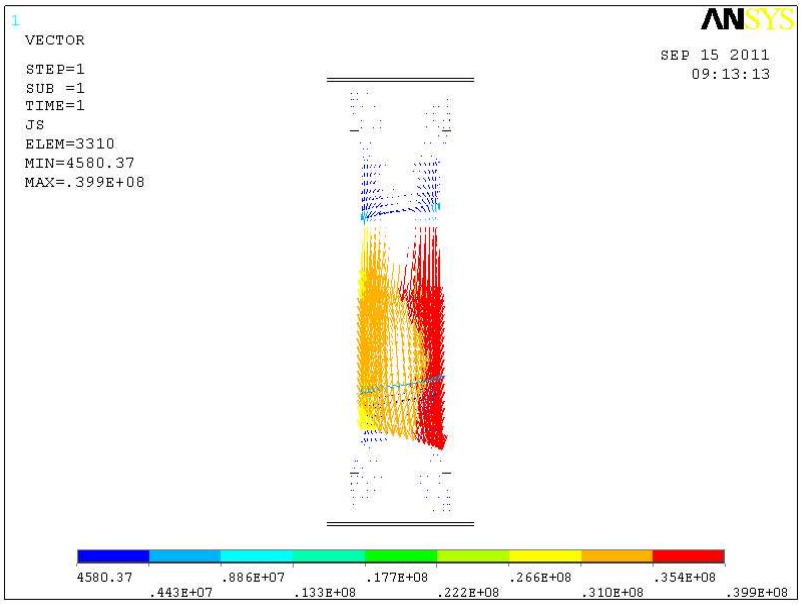

Figure 9 Current Distribution for Resistive Solution at 400 kA and TPF=1.35

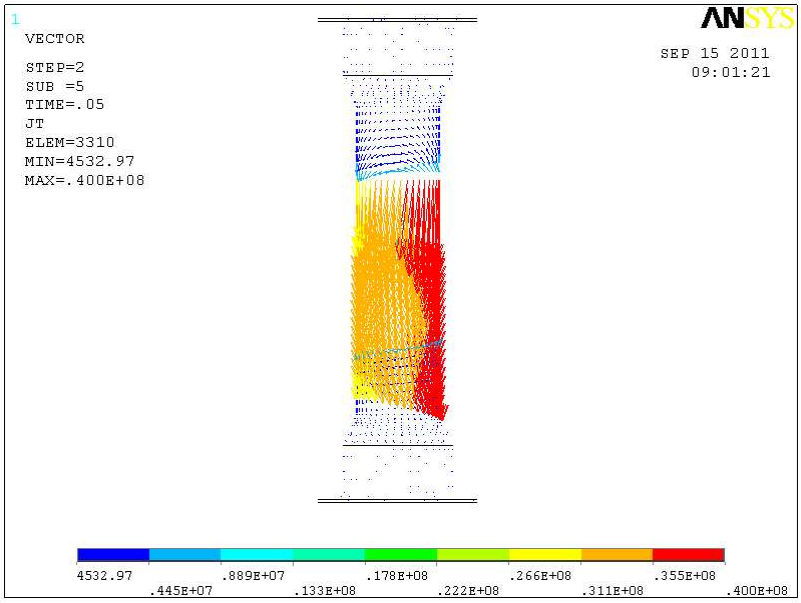

Figure 10 Current Distribution for Slow Quench at max total current is fairly resistive

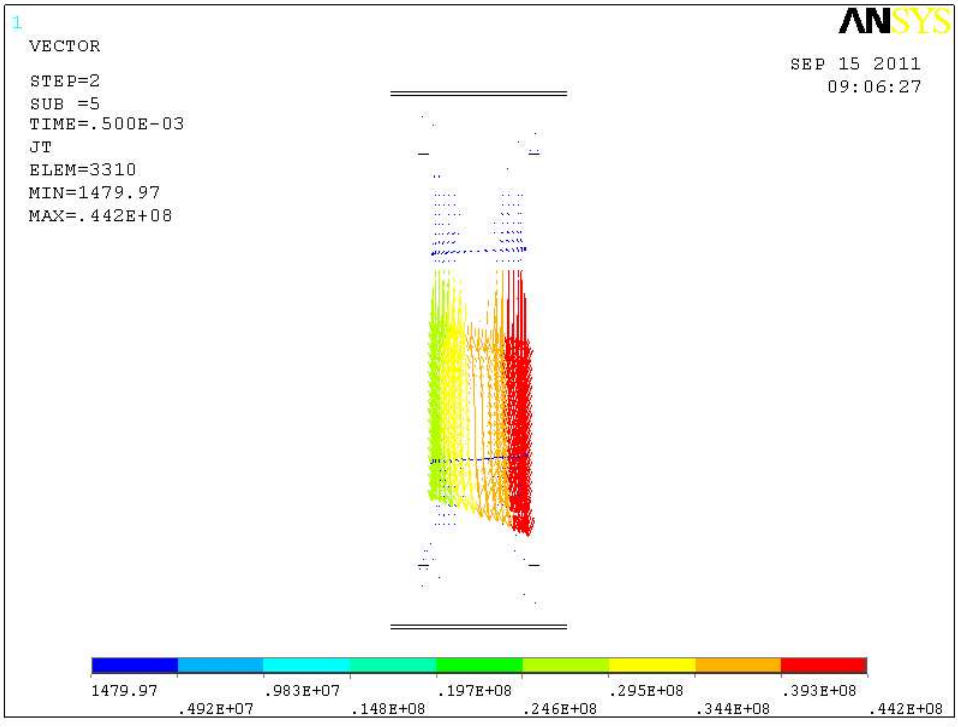

Figure 11 Current Distribution for Fast Quench at max total current show higher peaking

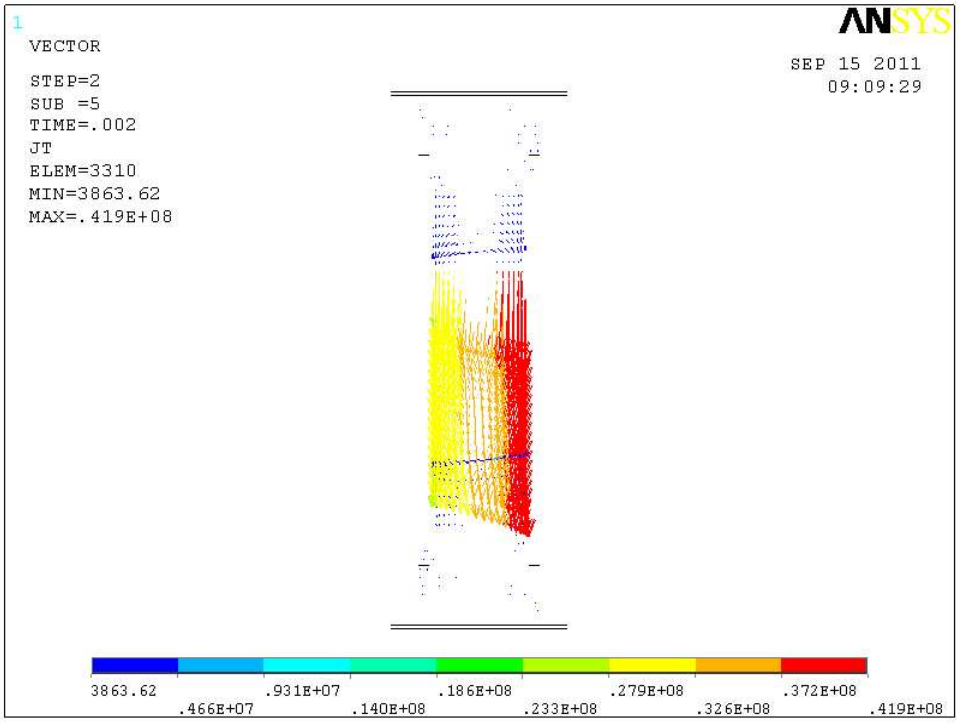

Figure 12 Current Distribution for Medium Quench at max total current

.

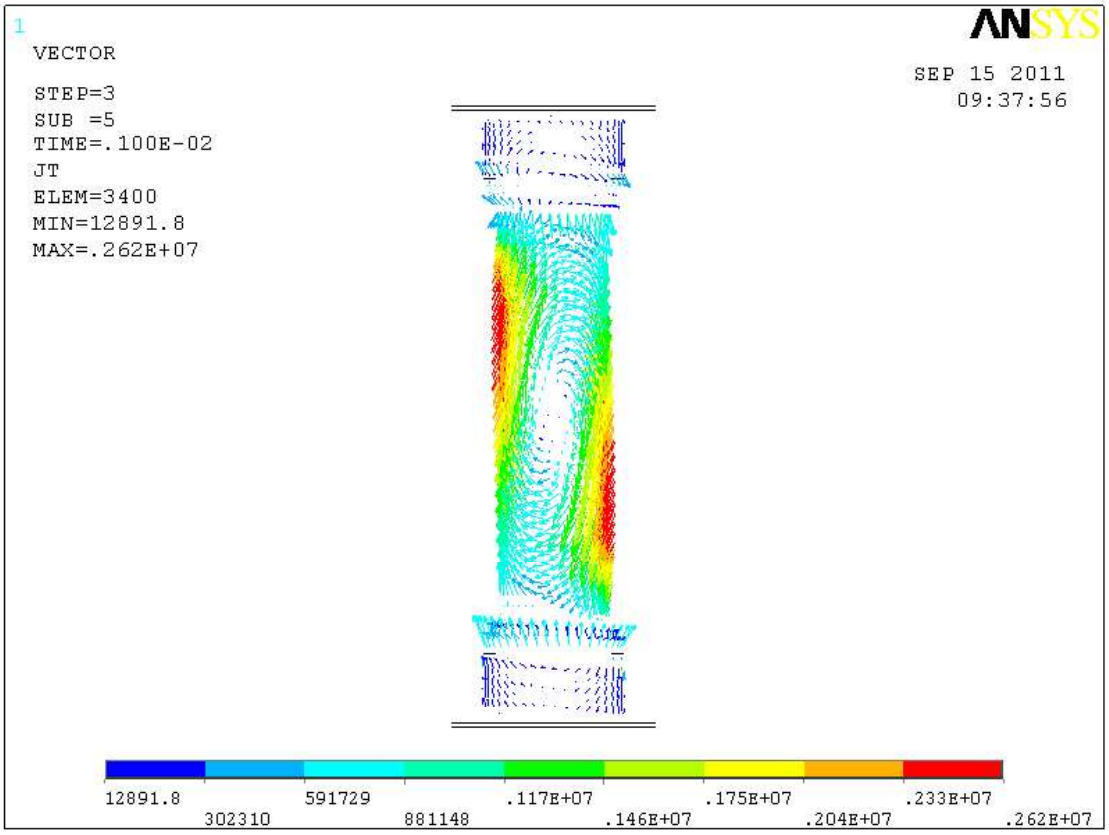

Figure 13 Halo distribution at end of triangular waveform where net poloidal current is zero. Circulating eddies persist.

The vertical halo currents flowing in the CS interact with the TF field producing local radial forces. If the current distribution is uniform, these radial forces produce hoop stresses within the CS but no net force since forces on opposite sides of the CS oppose each other. The peaked current distribution seen immediately following the halo current strike results in an imbalance in the load distribution as well which must be taken out by any structure supporting the CS. This imbalance is found to be significant as seen below resulting in a max net force of 146 kN (32,0820 lbs).

Based on recent guidance from Stefan the TPF at the strike point was adjusted such that the TPF at the midplane is 1.35 (the strike point needed to be increased to 1.60). This increased the net forces on the CS. The 250 kN is very close to the estimated value obtained by assuming a constant TPF of 1.35 over the +/- 0.6m height. Note this change is included in the subsequent structural analysis but not reflected in figure 14 below.

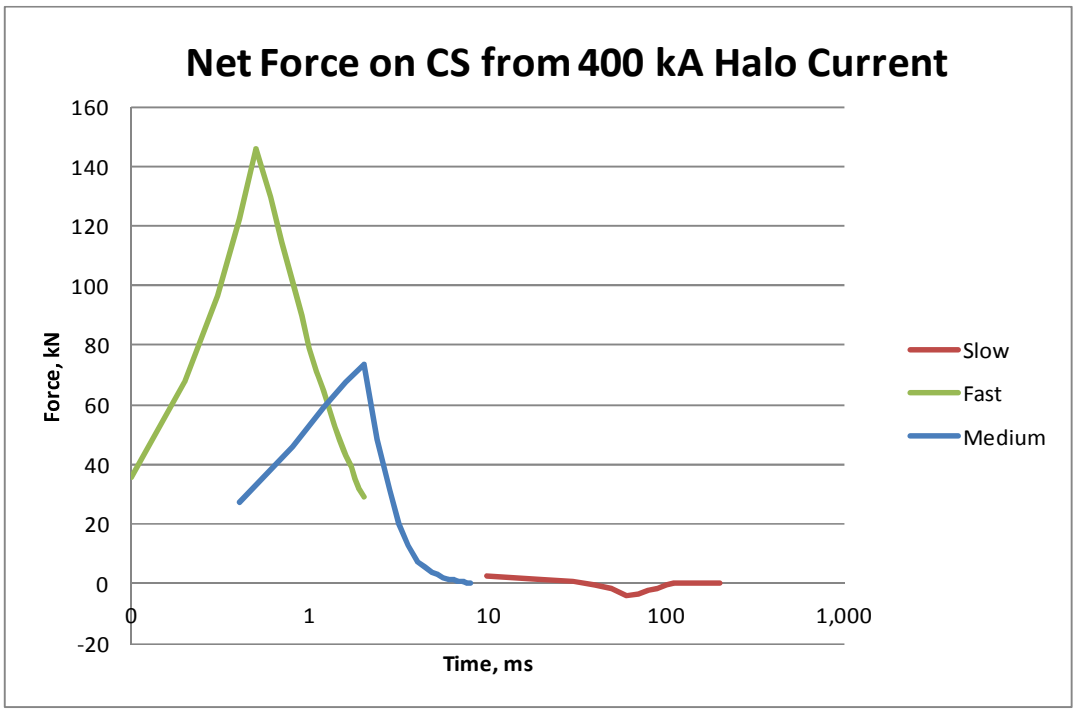

Figure 14 Net Force Transient on CS from Slow, Fast and Medium Current Quench Halos. Log scale used to expand different time scales.

The above forces must be reacted by the based support pedestal and the bellows at the top of the CS. A dynamic response of the CS was run for each scenario to calculate these reaction loads and displacements as well as to evaluate the transient stresses.

To properly capture the dynamic response, the masses of the ATJ tiles and PF1a&b where included by using effective densities of the top, middle and bottom sections of the CS. The table below summaries the results.

Increase effective density of CS Top & Bot to account for added mass from pf1a&b							
Assumes all mass added to CS Inconel Casing							
Section	Inc Vol	Inc Mass	Tile Vol	Tile Mass	Pf1a&b Mass	Total Mass	**Inc Eff Density**
	m3	kg	m3	kg	kg	kg	**kg/m3**
Top	0.03677	310.3	0.06257	110.1	1000.0	1420.5	**38631.0**
Mid	0.02487	209.9	0.07675	135.1	0.0	345.0	**13871.4**
Bottom	0.03677	310.3	0.06257	110.1	1000.0	1420.5	**38631.0**
Total	0.09841	830.6	0.20189	355.3	2000.0	3185.9	
Density							
Inconel	8440	kg/m3					
ATJ	1760	kg/m3					

Halo Current Analysis of NSTX CS

The damping coefficients were obtained from Peter Titus. The Rayleigh Damping coefficients alpha=12.56 and beta=8.e-6 were based on the conservative assumption 0.5% overall damping with a lowest natural frequency mode of 200 hz.

A bellows spring constant of 204,200 lbs/in was obtained from Pete Rogoff. Len Myatt combined this with the stiffness of the bumpers (which were added to the design to limit lateral motion of the CS) and VV and calculated an effective stiffness of 420,000 lbs/in to ground.

The first set of plots which follow (Figure 15 thru Figure 31) are based on the CS rigidly supported at its base. They show the displacement and forces at the bellow, the forces and moments at the base support and the peak tresca stress (aka stress intensity in ANSYS) transient values and max distribution for the slow, fast and medium quench scenarios. The run times were the same for each to compare 'ringing' of the CS and the reactions.

One observation is that although the net loads differ significantly as do the reactions, the peak stresses are not significantly different 42 - 44 MPa. The peak stress is driven by the hoop stress near the halo injection points which dominate.

The max displacement at the bellows is shown to be 0.5 mm for both the fast and medium quench. The corresponding max lateral force is 18,000 N (4,046 lbs).

The base support reacts most of lateral load, 140 kN (31,400 lbs), as expected since it is rigidly held. There is also a reaction moment about the center of the base flange of 90 kN-m (66,800 ft-lbs) for the worse case fast quench scenario.

Note this first set of outputs was the initial analysis results where the CS is rigidly support at its base. This rigid mount over predicts the reaction loads. To remove some of this conservatism the analysis was rerun with the rigid support moved to bottom of the G10 washer of the pedestal support, approximate 1 m in elevation below the CS. Figures 33 thru 38 again) show the displacement and forces at the bellow, the forces and moments at the base support and the peak tresca stress (aka stress intensity in ANSYS) transient values and max distribution for ??

Slow Quench Results

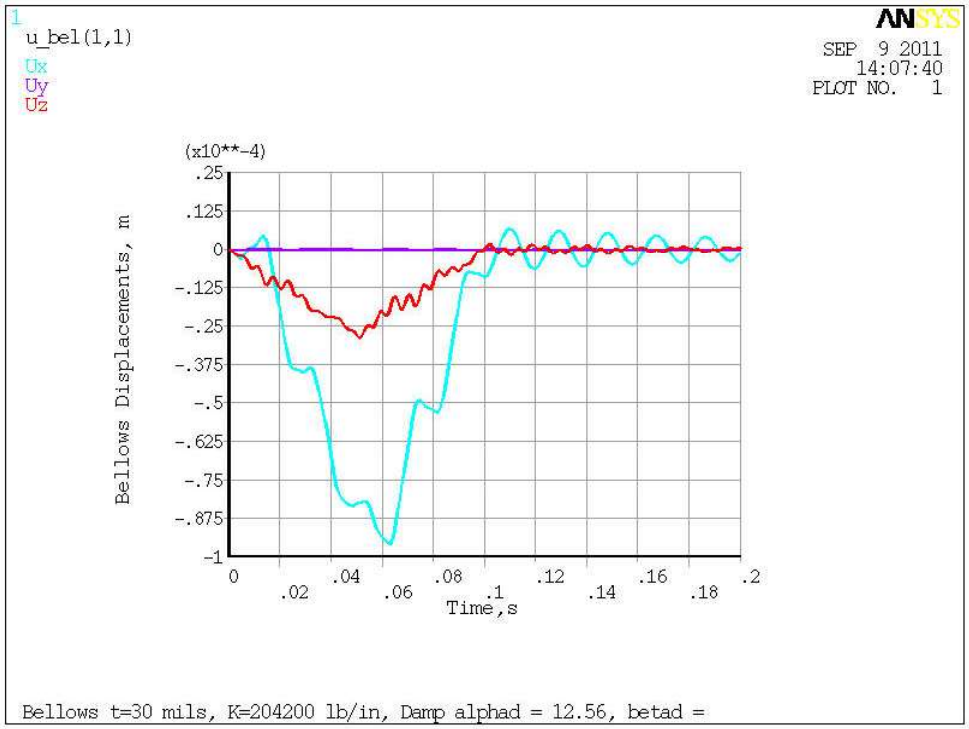

Figure 15 CS Displacements at Upper Bellows Displacement during Slow Quench

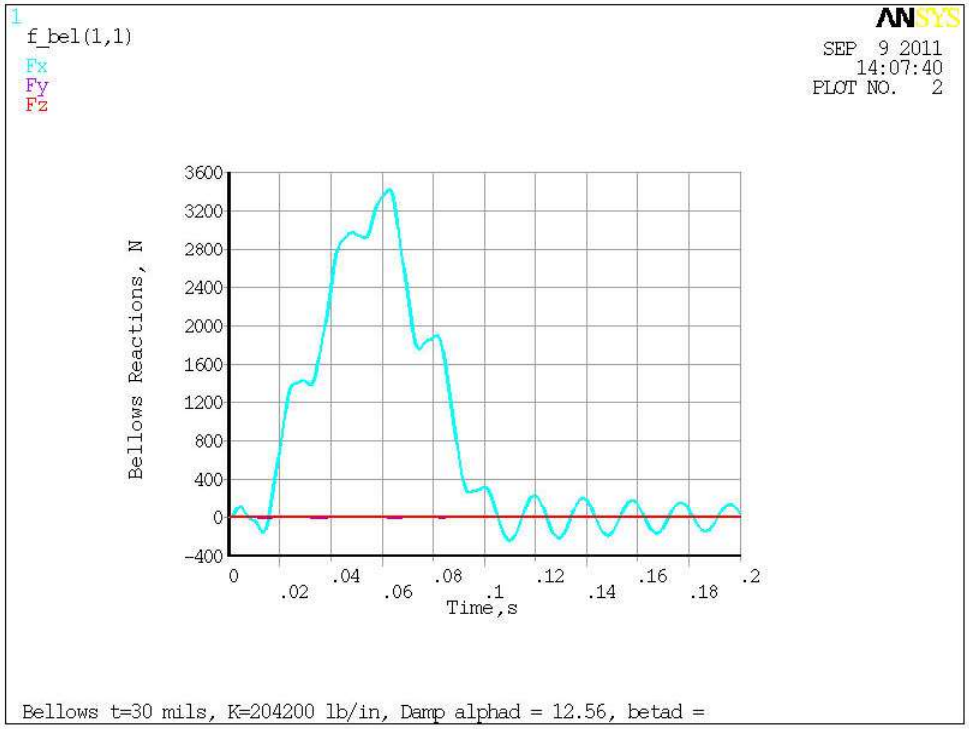

Figure 16 CS Reaction Loads at Upper Bellows during Slow Quench

Slow Quench Results (cont'd)

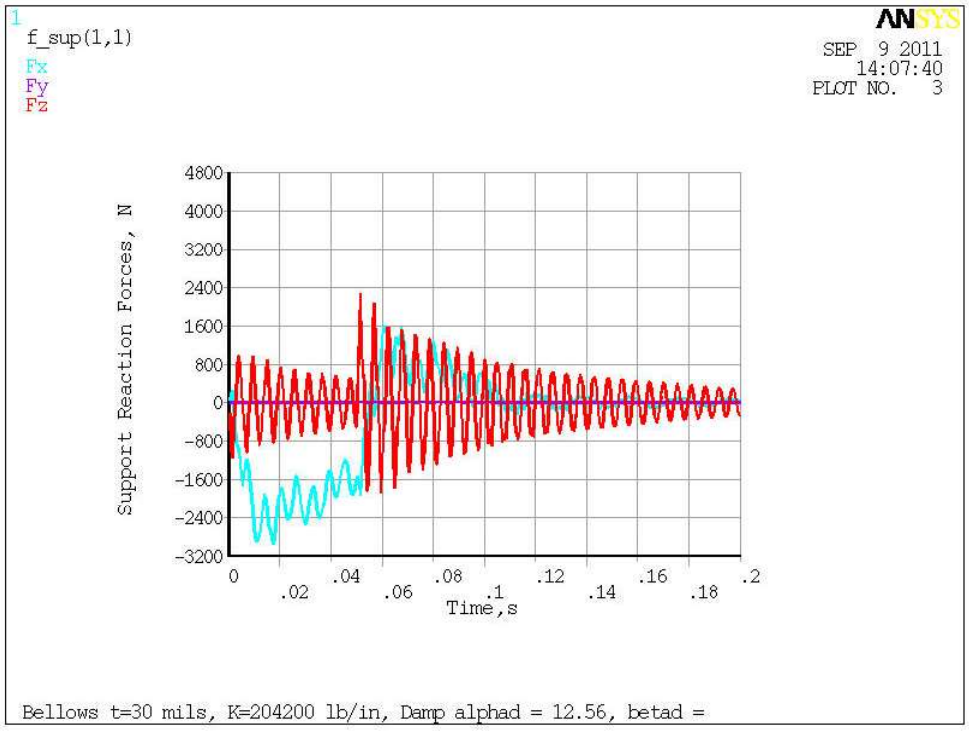

Figure 17 CS Reaction Forces at Base Support for Slow Quench

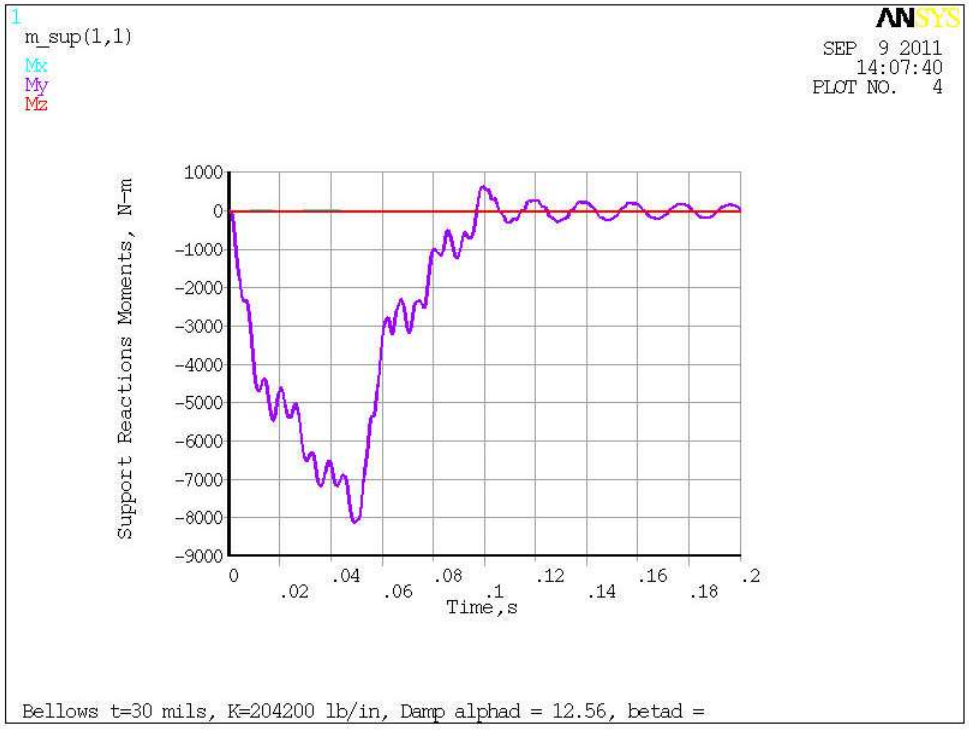

Figure 18 CS Reaction Moments at Base Support for Slow Quench

Slow Quench Results (cont'd)

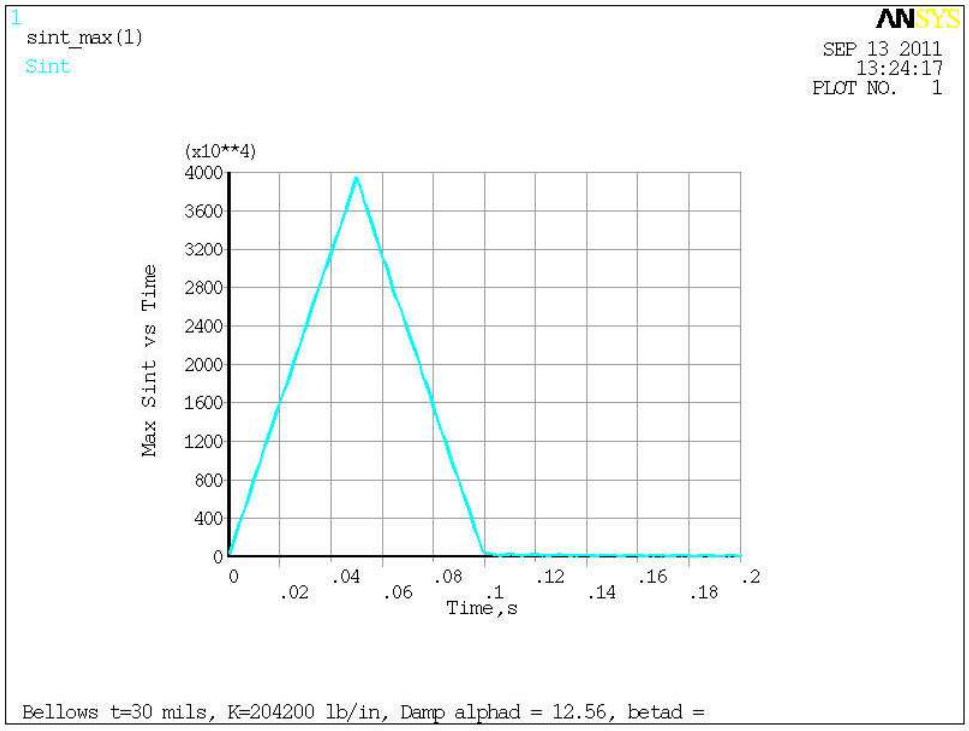

Figure 19 CS Max Tresca Stress for Slow Quench

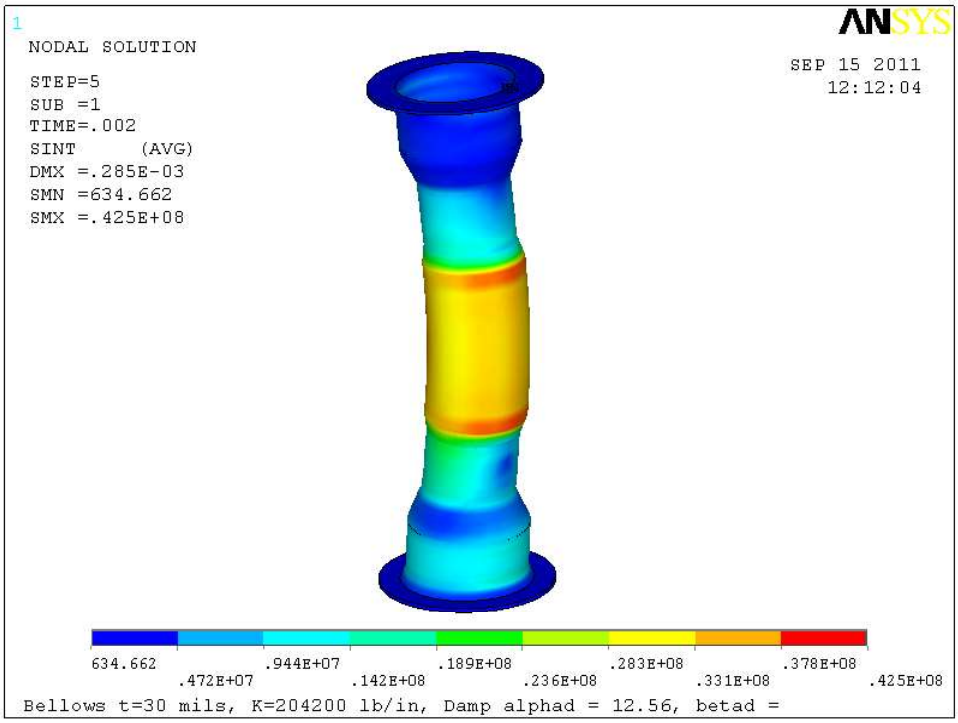

Figure 20 CS Tresca Stress Distribution at Max Value for Slow Quench

Fast Quench Results

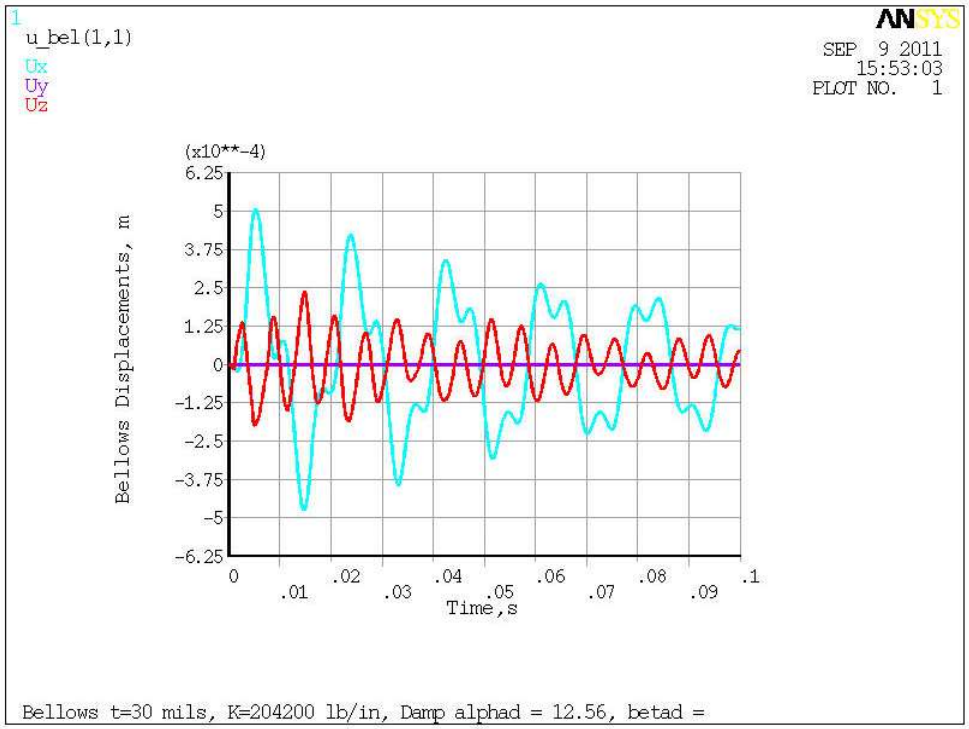

Figure 21 CS Displacements at upper Bellows Displacement during Fast Quench

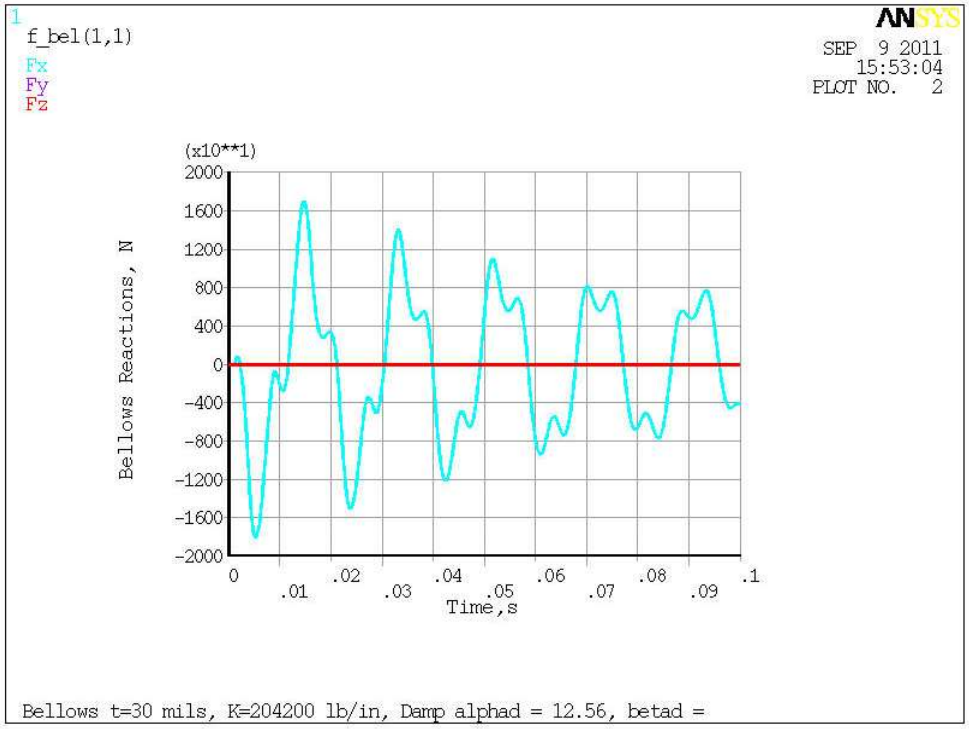

Figure 22 CS Reaction Loads at Upper Bellows during Fast Quench

Fast Quench Results (cont'd)

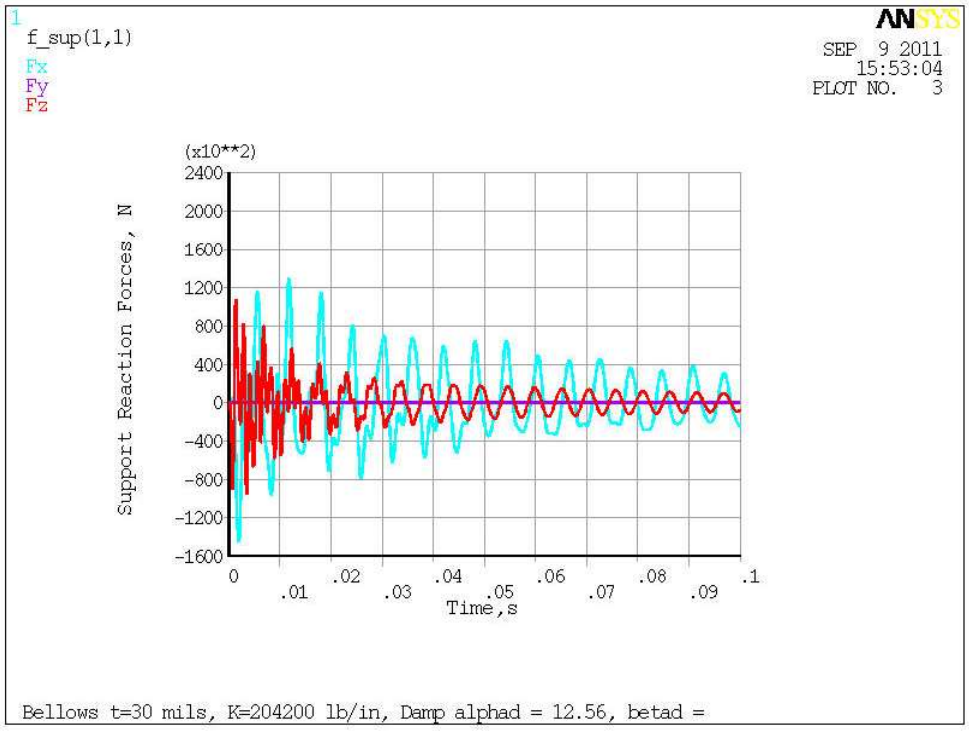

Figure 23 CS Reaction Forces at Base Support for Fast Quench

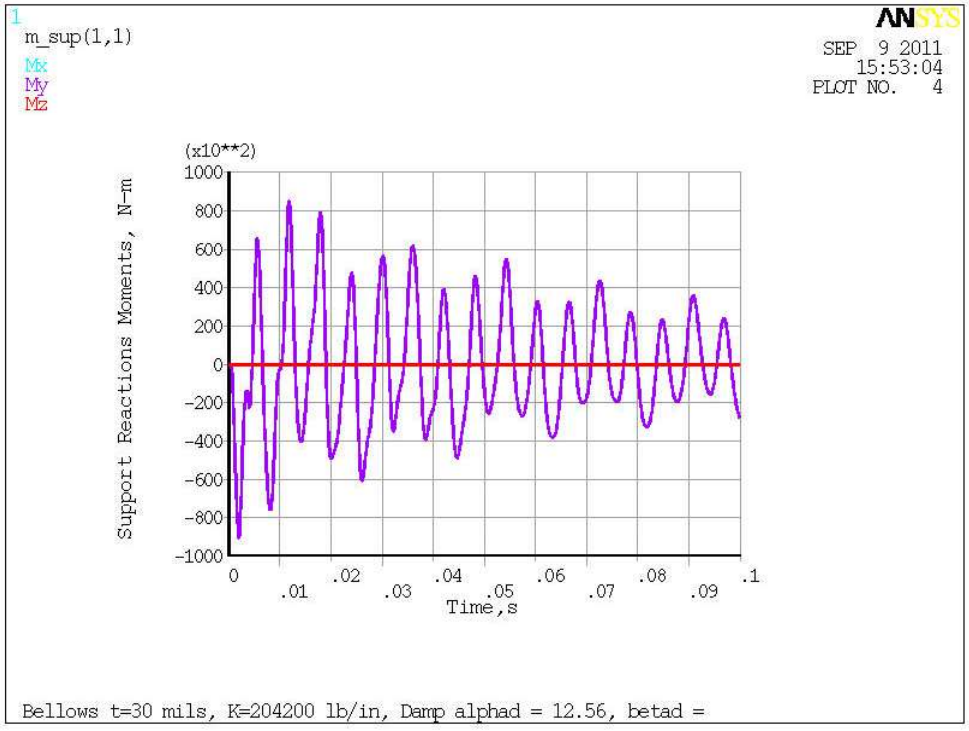

Figure 24 CS Reaction Moments at Base Support for Fast Quench

Fast Quench Results (cont'd)

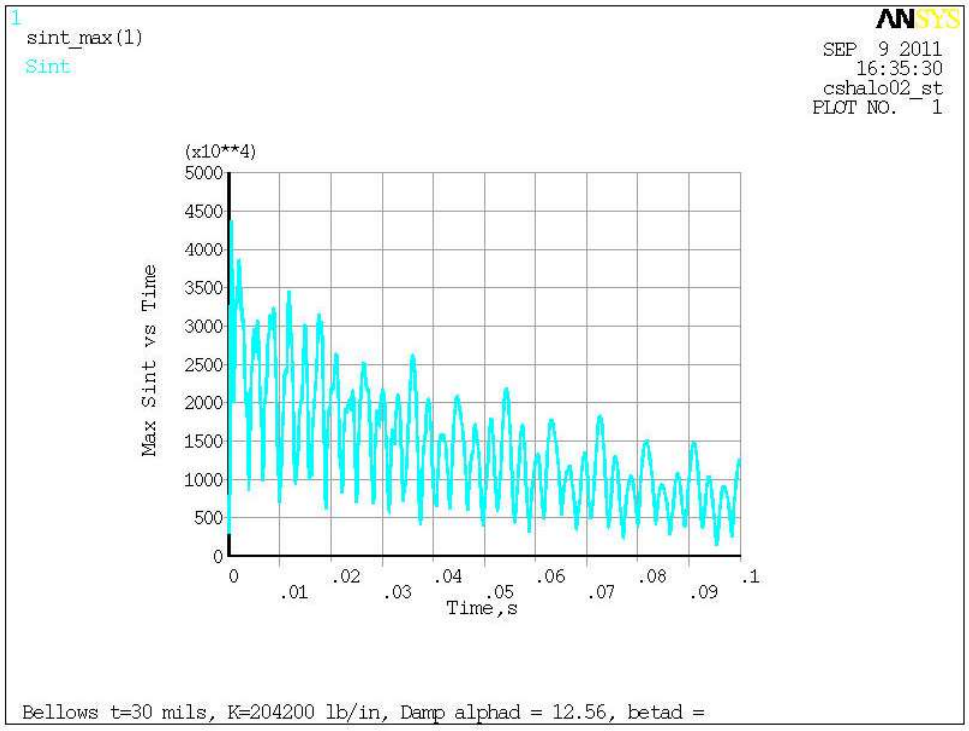

Figure 25 CS Max Tresca Stress for Fast Quench

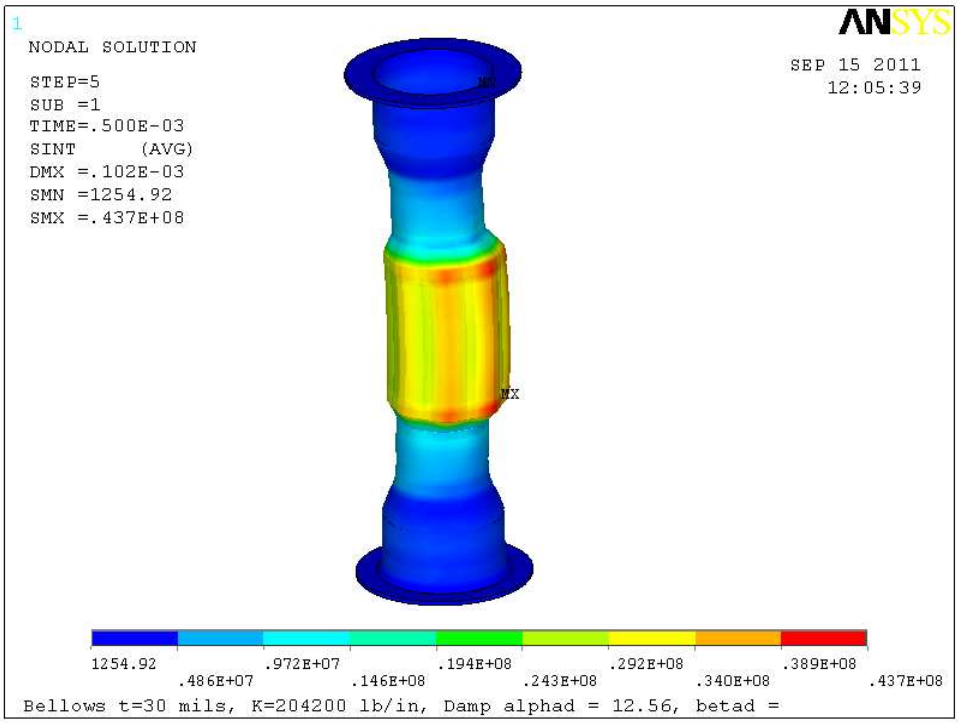

Figure 26 CS Tresca Stress Distribution at Max Value for Fast Quench

Medium Quench Results

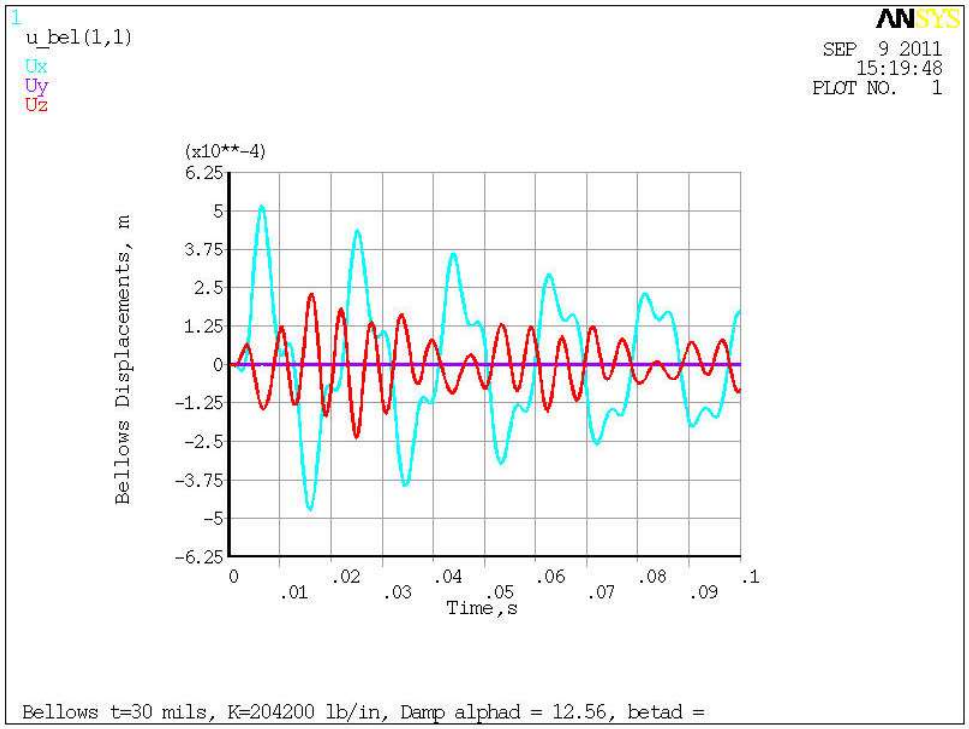

Figure 27 CS Displacements at Upper Bellows Displacement during Medium Quench

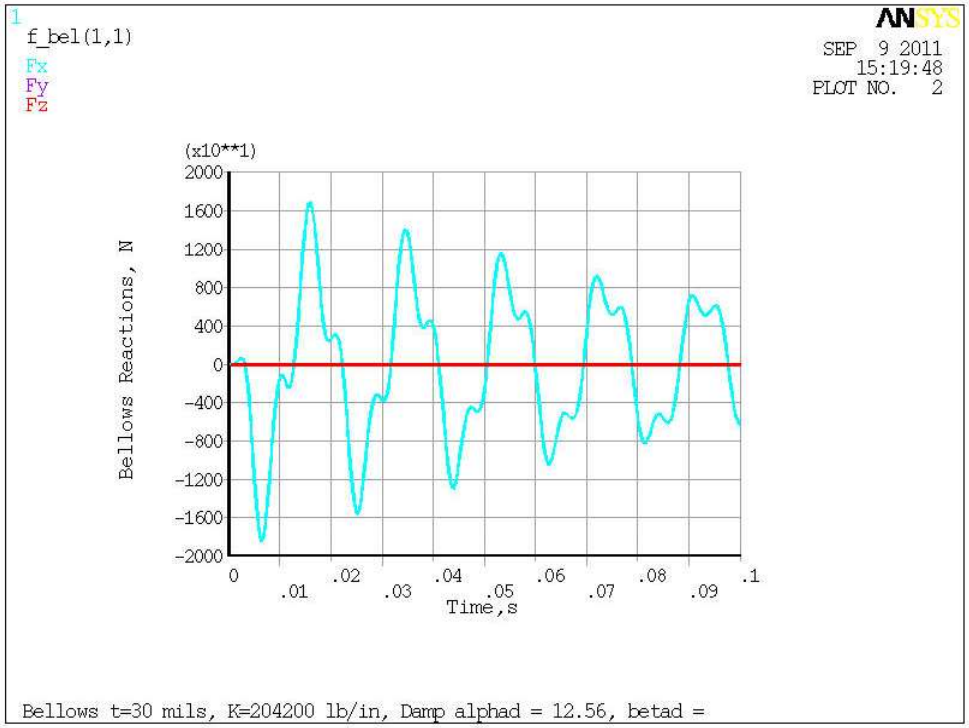

Figure 28 CS Reaction Loads at Upper Bellows during Medium Quench

Medium Quench Results (cont'd)

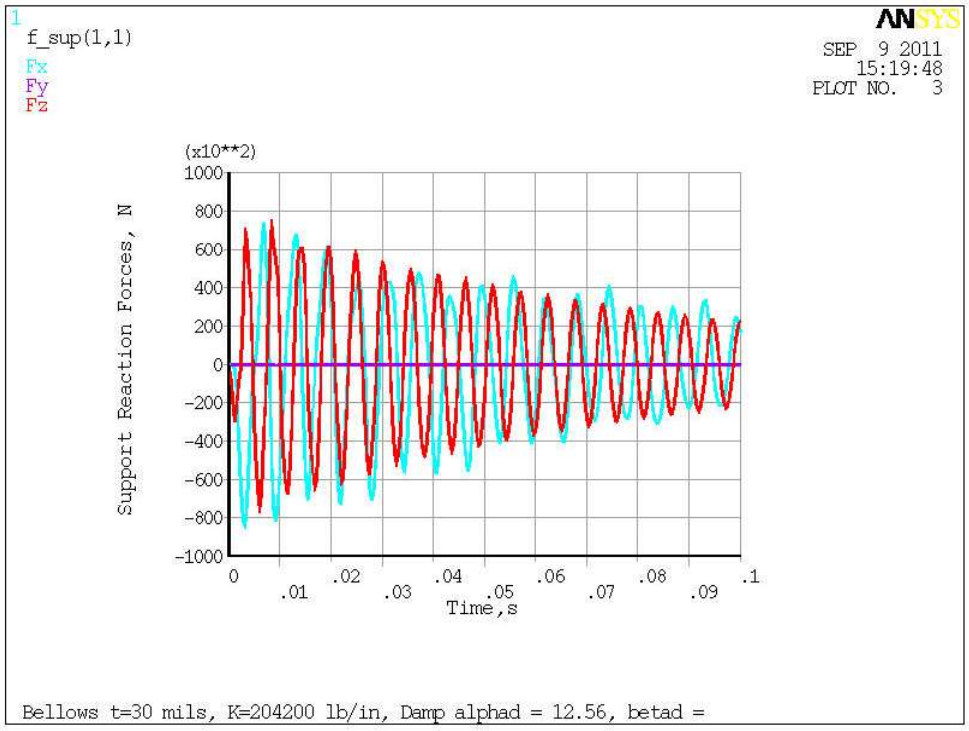

Figure 29 CS Reaction Forces at Base Support for Medium Quench

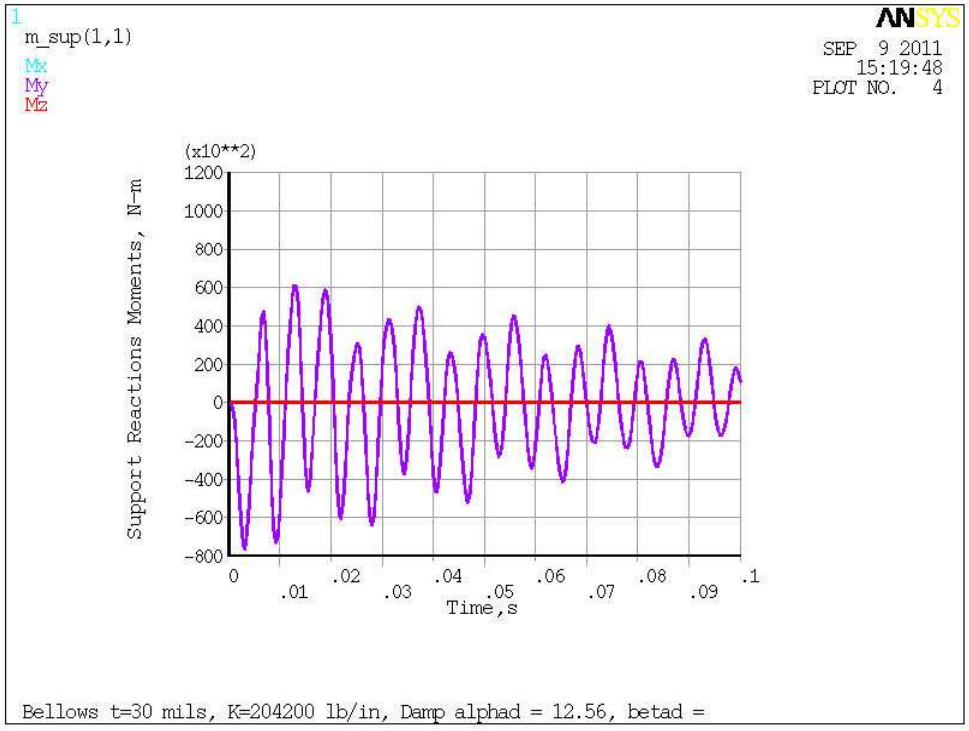

Figure 30 CS Reaction Moments at Base Support for Medium Quench

Medium Quench Results (cont'd)

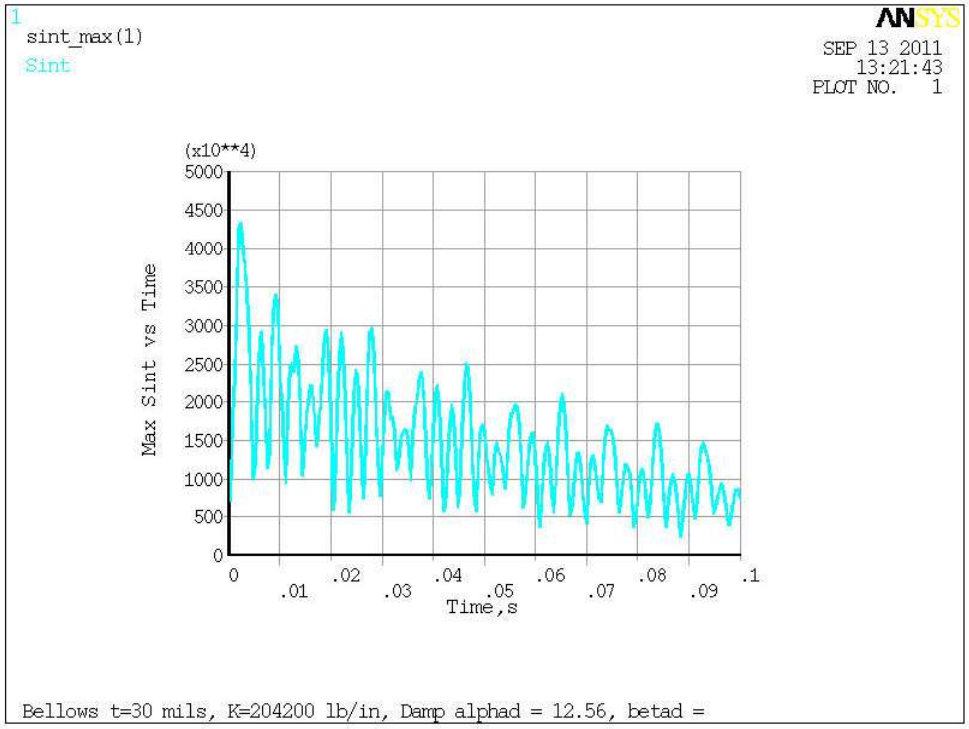

Figure 31 CS Max Tresca Stress for Medium Quench

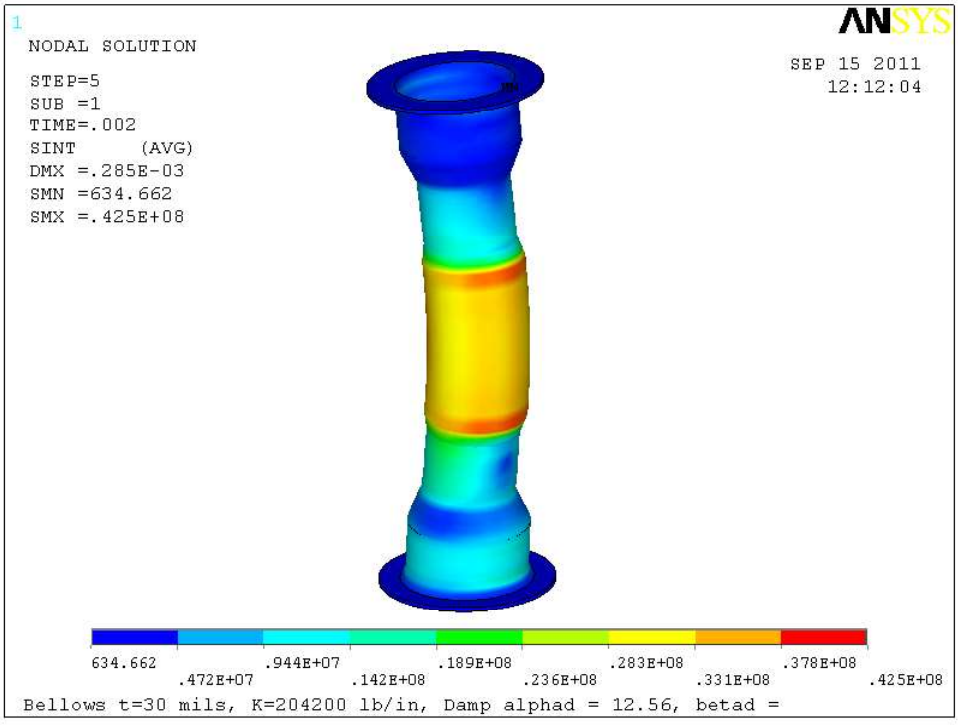

Figure 32 CS Tresca Stress Distribution at Max Value for Medium Quench

Results with G-10 washer at based of pedestal support

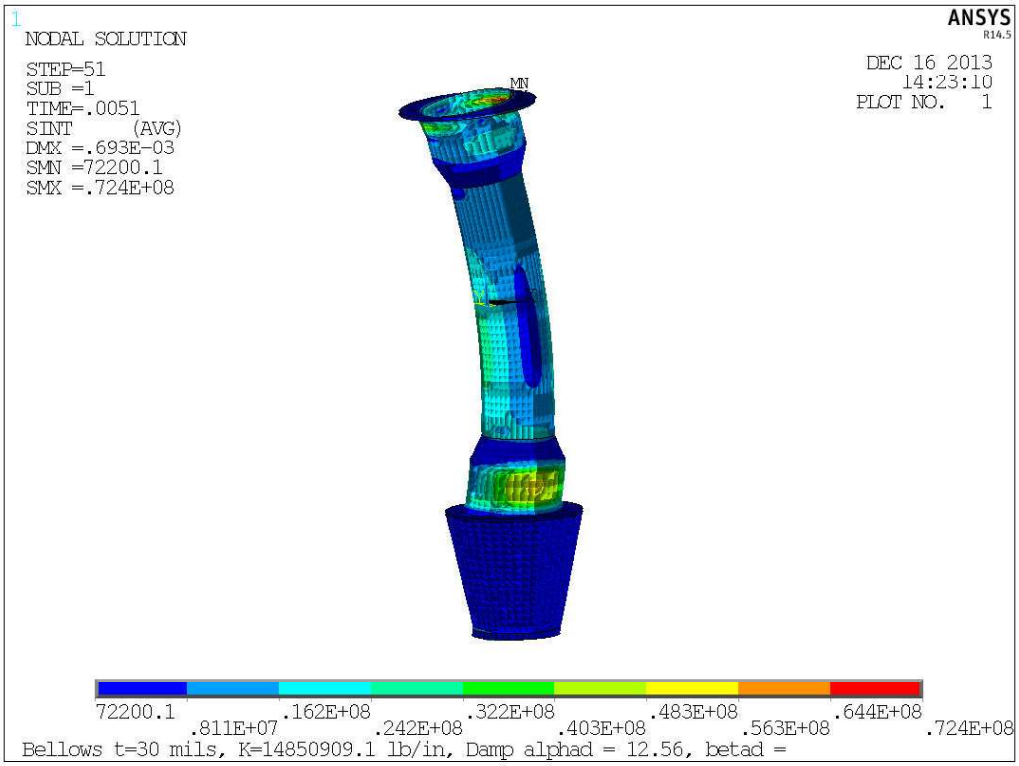

Figure 33 Stress Intensity distribution when peak occurs at 5.1 ms

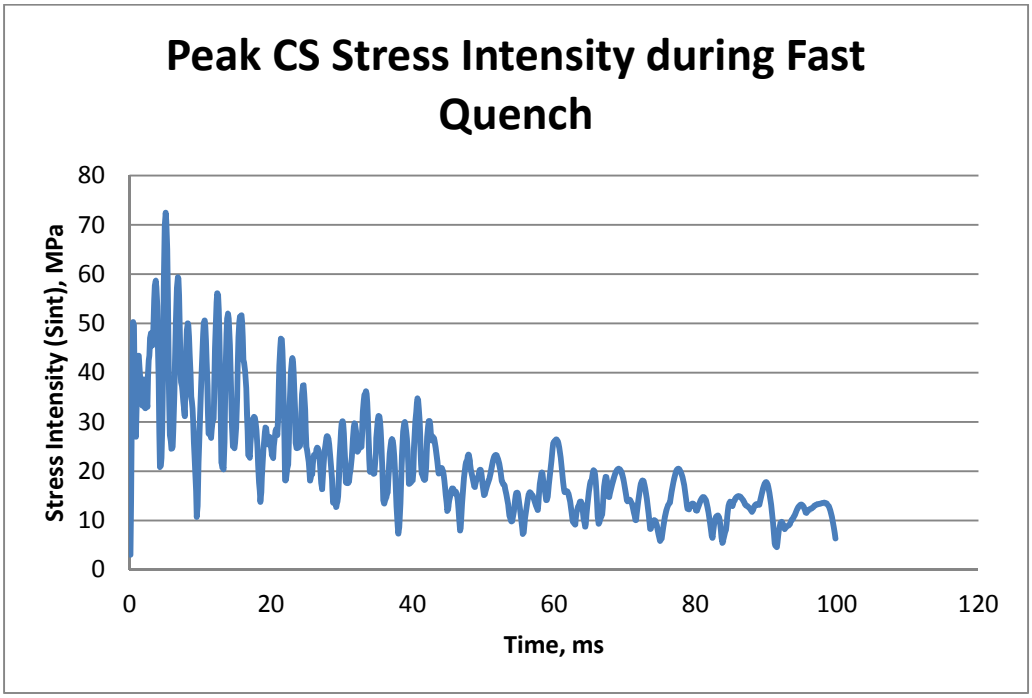

Figure 34 Peak CS Stress during Transient

Bellows Reaction Loads

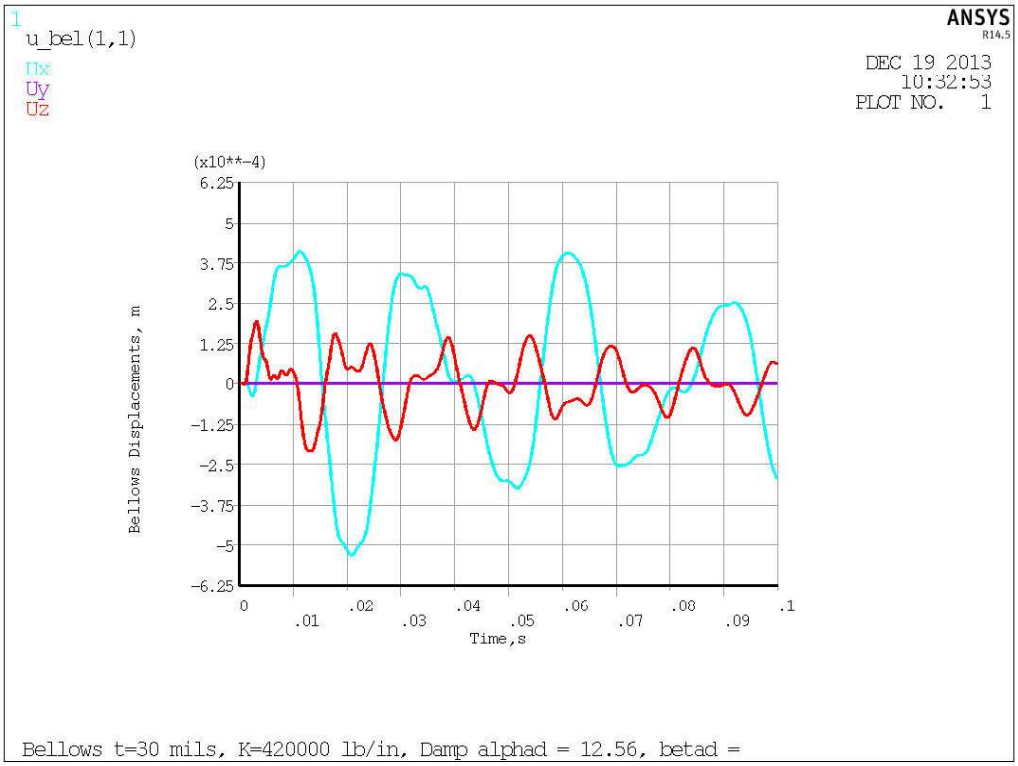

Figure 35 Bellows Displacements

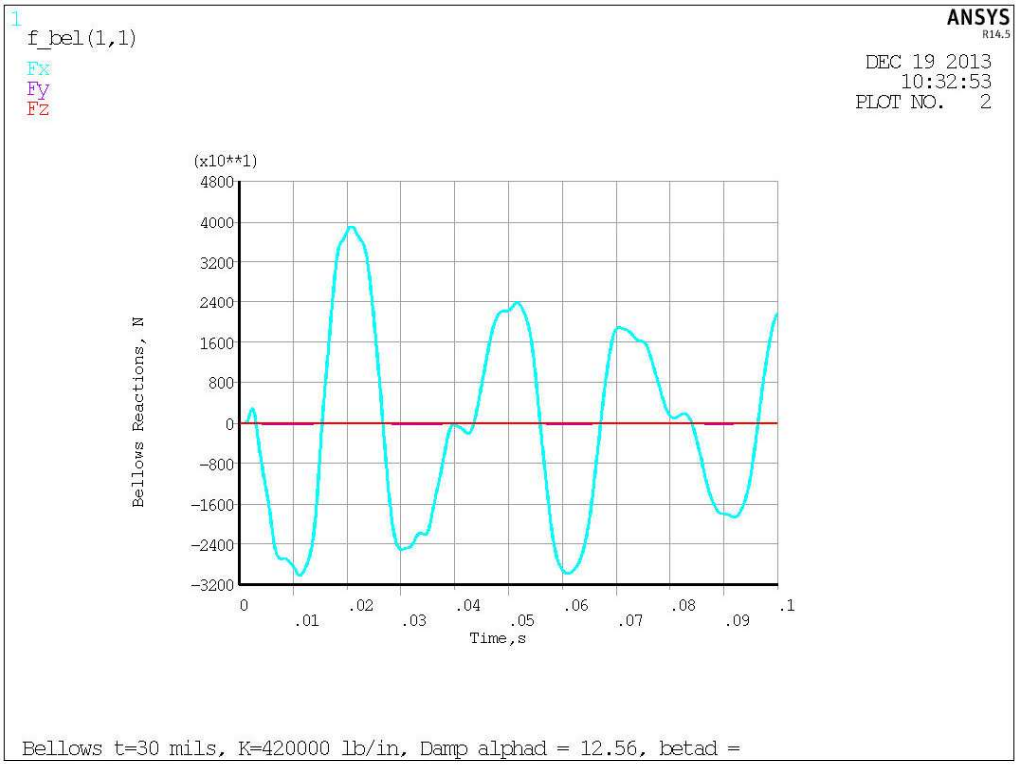

Figure 36 Bellows Reaction Loads

Lower Support Reaction Loads (moments about point [0,0,-2.7])

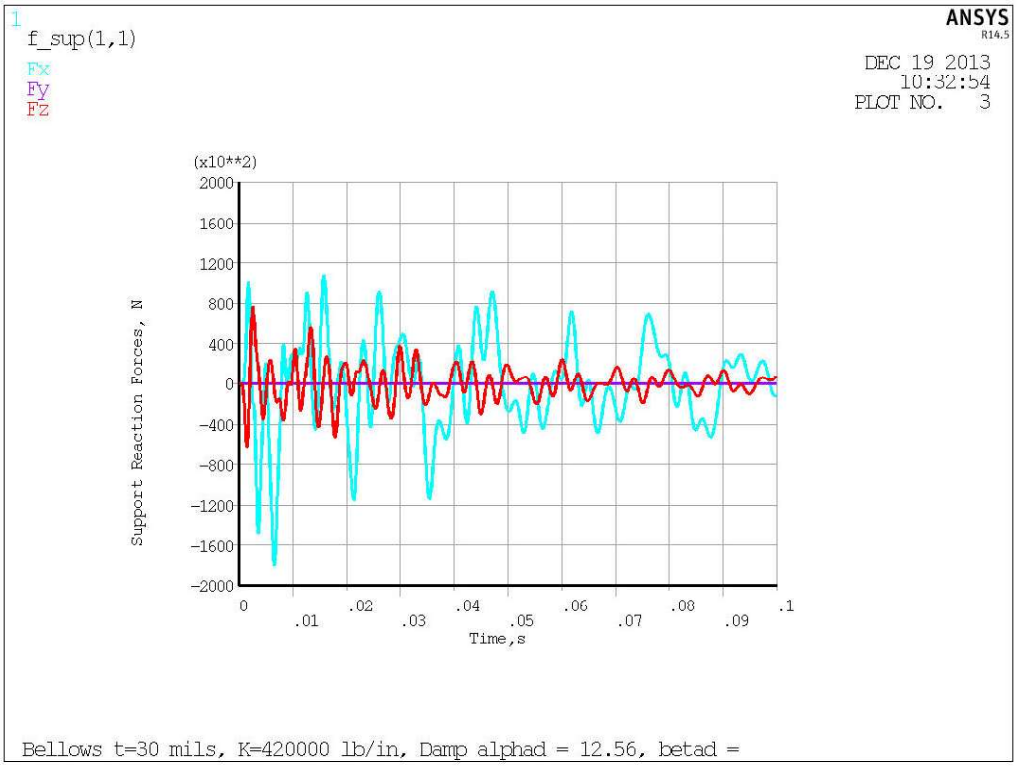

Figure 37 Lower Support Reaction Loads

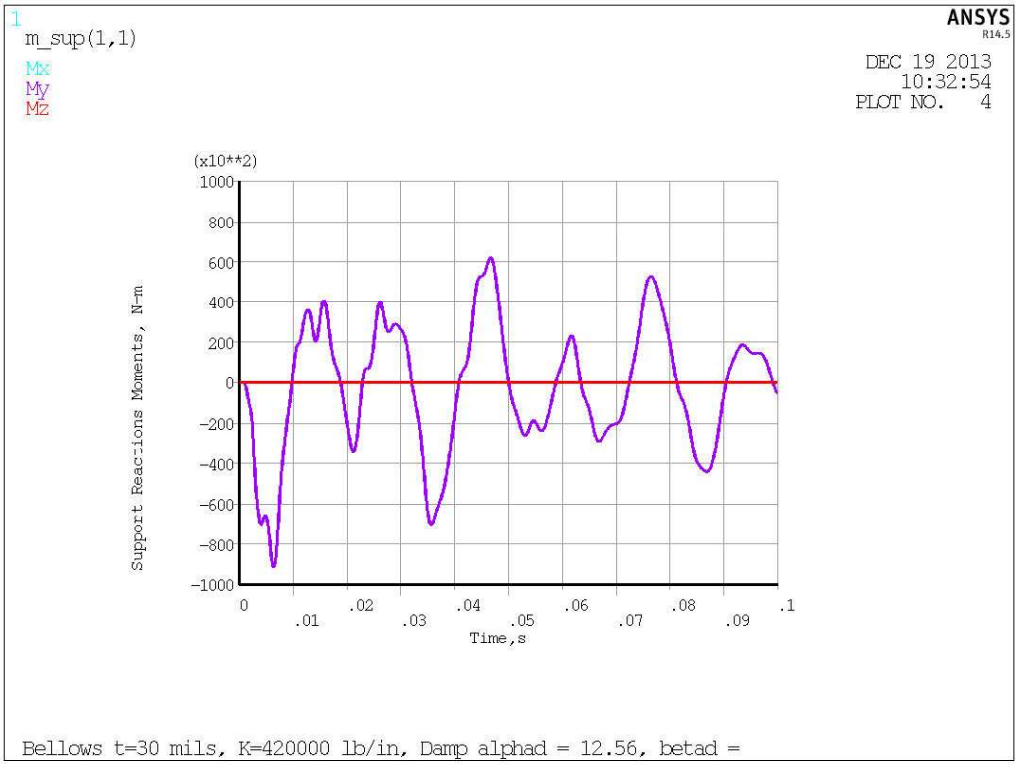

Figure 38 Lower Support Reaction Moments about [0,0,-2.7]

Reaction Loads at CS Base/Top of Lower Support (moments about point[0,0,-1.7])

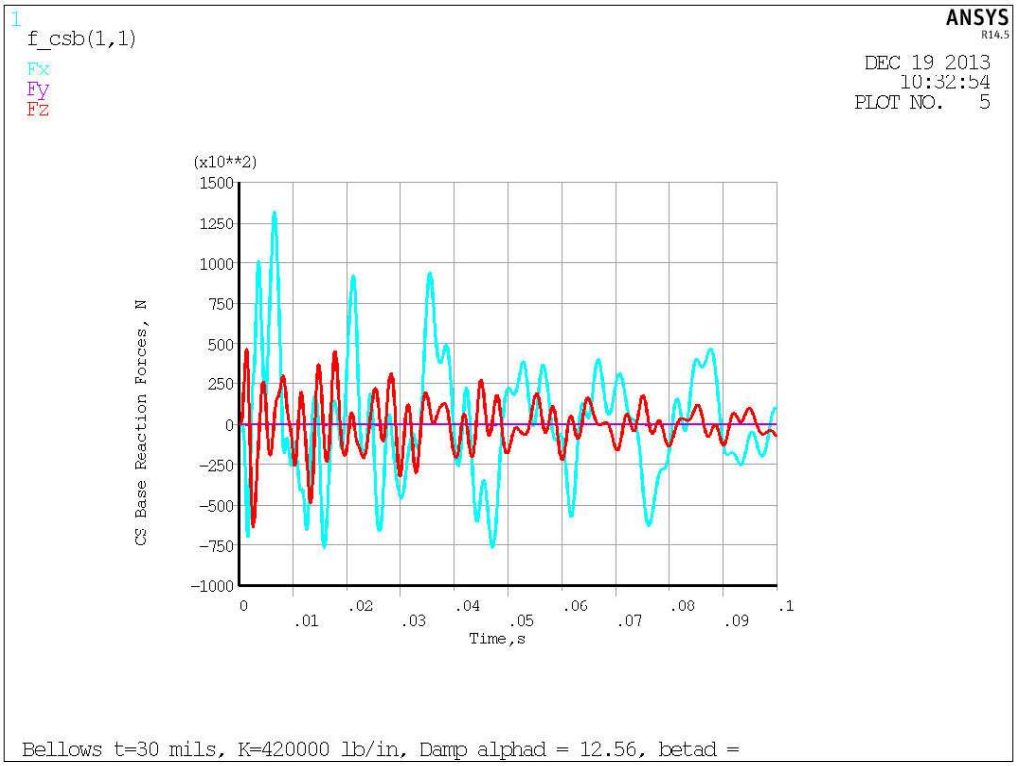

Figure 39 Reaction Forces at base of CS

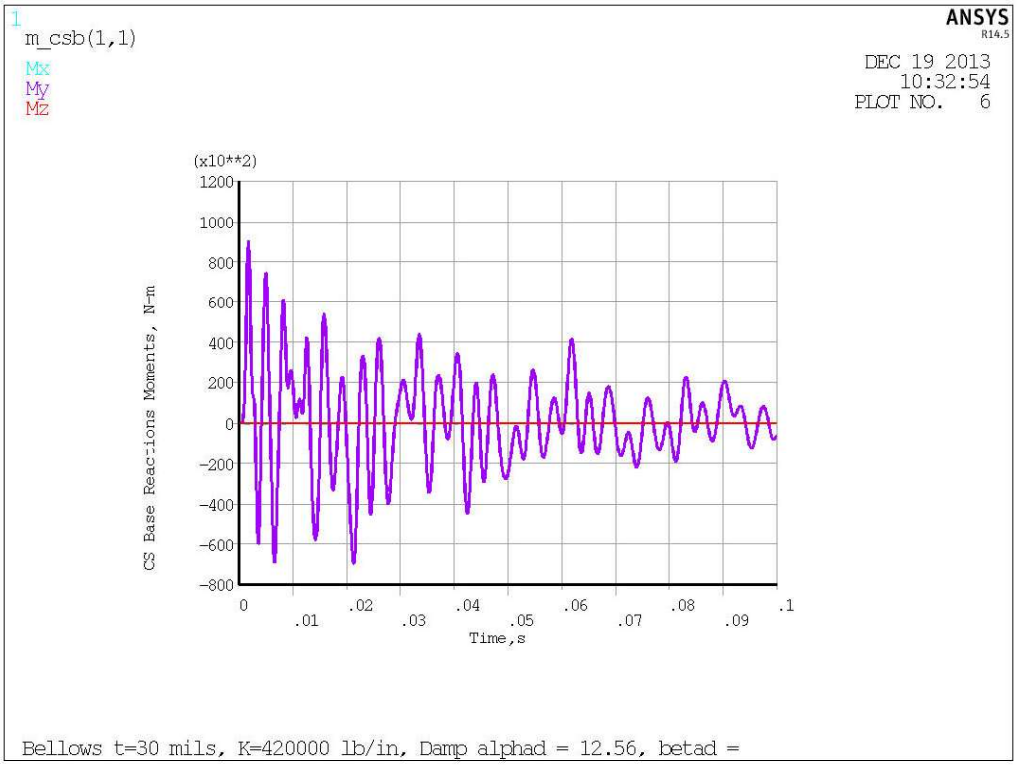

Figure 40 Reaction Moments at base of CS

Halo Current Analysis of NSTX CS

Summary

The results presented here showed the inductive effects to be significant for the halo model assumptions presented. The slow quench (100 ms) has a fairly resistive response leading to more current redistribution, lowering the toroidal peaking factor to 5% at the midplane, and lower net radial forces. The fast quench (1 ms) shows much less current redistribution with the toroidal peaking factor the midplane still 22% and much higher net radial forces (140kN). The decision by physics to apply the TPF to the midplane and not the strike point drove the net radial force up to 250 kN. The max lateral displacement at the bellows is 0.5mm and reactors a small part of the applied load whereas the base support must be capable of reacting the full 250kN load. The stresses are shown to be fairly independent of the scenario. At the revised loading the max tresca stress is 73 MPa, well within allowables.

Adding the compliant G10 plate and structure sitting on the TF flags reduces the moment (now measure at the G10, z=-2.7m) to a peak of 95 kN-m during the dynamic response. The net lateral force drops to 180 kN. The bellows/bumper reaction drop slightly to 32 kN and again is not in phase with the reaction load at the base (see figures)

The peak vertical load at the interface of the base of the CS and top of the lower support is lower (~60 kN) than at the bottom of the lower support (~80 kN). The moments are about the same (~95 kN-m) but occur at different times. The numbers are extracted using fsum on the interface nodes with the lower support elements and are the total force (static + inertial + damping).

References

1) NSTX_CSU-RQMTS-GRD General Requirements Documents, Rev 3
2) Design Point Spreadsheet “NSTX_CS_Upgrade_100504.xls”
3) ProE Model of Center Stack Tiles - aj_center_case_analysis_rev2.asm
4) Spreadsheet of Disruption Data - Disruption_scenario_currents_v2.xlsx, by Jon Menard, received 7/2/2010
5) Discussions with Stefan Gerhardt on modeling of halo currents for NSTX
6) Bellows Qualification Calc # NSTXU CALC 133-10-00, Peter Rogoff’
7) NSTX Upgrade Center Stack Casing and Lower Skirt Stress Summary NSTXU-CALC-133-03-00 Peter Titus
8) Email Sept 9 2011 containing recommendations for damping values, including Regulatory Guide 1.61 as an attachment. Included in Attachment A
9) MODELLING OF THE TOROIDAL ASYMMETRY OF POLOIDAL HALO CURRENTS IN CONDUCTING STRUCTURES N. POMPHREY, J.M. BIALEK_, W. PARK, Princeton Plasma Physics Laboratory, Princeton University, Princeton, New Jersey, NJ

Halo Current Analysis of NSTX CS

Attachment A

Sent Friday Sept 9
Attached are a couple of references on the appropriate damping values for structures.
Reg Guide 1.61

There is no listing for tokamak centerstack casings. You have to use some judgment. I would argue that based on reg. guide 1.61 and the fact that the CS casing has insulation, and tiles frictionally clamped to it, that a pretty high value (~2 to 3%) would be appropriate, but because we don't have test data for our structures, we have been using .5 % -Peter